MEASUREMENT OF SPECTRAL LINE PROFILES IN DENSE PLASMAS

by

HARRY GORDON JAMES

B.Sc., Queen's University, 1963

M.Sc., University of British Columbia, 1965

A THESIS SUBMITTED IN PARTIAL FULFILMENT OF

THE REQUIREMENTS FOR THE DEGREE OF

DOCTOR OF PHILOSOPHY

in the department

of

PHYSICS

We accept this thesis as conforming to the

required standard

THE UNIVERSITY OF BRITISH COLUMBIA

March, 1968

In presenting this thesis in partial fulfilment of the requirements for an advanced degree at the University of British Columbia, I agree that the Library shall make it freely available for reference and study. I further agree that permission for extensive copying of this thesis for scholarly purposes may be granted by the Head of my Department or by his representatives. It is understood that copying or publication of this thesis for financial gain shall not be allowed without my written permission.

Department of PHYSICS

The University of British Columbia
Vancouver 8, Canada

Date APRIL 3, 1968

ABSTRACT

The spectra emitted by a pulsed-arc discharge have been photographed with a medium resolution spectrograph to obtain Stark broadened line images measurable for both width and shift. Plasmas with densities near $10^{17} cm^{-3}$ and temperatures of about 2.6 ev were produced by subjecting Argon - Nitrogen mixtures to a square current pulse. Light from the discharge was shuttered by a rotating mirror system so that the plasma was photographed in an interval during the current pulse when the plasma had optimal conditions for measurement. A technique in which the spectral lines from a standard source are photographed on the same plates as the plasma lines has been devised for calibrating the measurement routine and for facilitating shift measurements. Stark parameters were obtained by scanning the plates on a precision comparator.

Nineteen ArII lines and six NII lines were studied. For Argon, the agreement with other experimental results is satisfactory but the theory is inadequate. Similarly, the NII theory does not predict the values measured here. On the other hand, some of the qualitative predictions by the Impact theory about the line shape and about the common widths and shifts of lines in the same multiplet have been confirmed. The experiment on the NII lines also reveals advantages of the present technique over other methods for obtaining Stark parameters.

TABLE OF CONTENTS

LIST OF TABLES

LIST OF FIGURES

ACKNOWLEDGEMENT

The author wishes to sincerely thank Dr. A. J. Barnard for his inspiration and supervision of the project.

In the course of the work, the author has benefitted from discussions with many of the staff and graduate school at U. B. C., and must express his indebtedness to the whole group. In particular, the help supplied by Mr. Hugh Campbell, whose familiarity with the apparatus was essential, and by Dr. Roy Nodwell, who criticized the manuscript, is hereby gratefully recognized.

Thanks are due for the Atomic Energy Control Board of Canada and the National Research Council of Canada for financial support of the laboratory in which the experiment was conducted.

Finally, the author expresses his thanks to his wife, Elsie James, for her total and patient support of the Ph.D. project.

CHAPTER 1 - INTRODUCTION

The theory of line broadening has been developing quite steadily over the last 75 years. During this period, real advances in the comprehensiveness and the applicability of the theory have been made by such illustrious workers as Lorentz, Michelson and Weisskopf. The study of spectral line shapes has always been interesting because it has been a useful area in which new concepts of the character of the atom could be both theoretically employed and then experimentally tested. The progress of the theory was directly dependent on the advent of the electro-magnetic theory, the quantum mechanical formalism and, more recently, the ideas of plasma kinetics.

Because line broadening theory involves so much basic physics, it provides a convenient basis for checking our concepts of the atom. But the interest in line broadening is not confined to the pure physics realm: once the physics is understood, experimentalists may apply the theory to the field of plasma diagnostics. In fact considerable attention is being given to the use of line broadening as a plasma diagnostic since, as Margenau and Lewis(1959) say, the use of spectroscopic equipment to analyse light emitted from a plasma seems to be the closest one can get to the ideal of the detached probe. Some plasmas are perturbed significantly by any kind of probe that interferes with them physically, while others

like celestial nebulae can only be understood through the radiation they emit. So, dependable line broadening concepts are a definite boon to the observer who wishes to make reliable measurements.

Atoms in a plasma so tenuous that they experience no interaction with their neighbours emit unbroadened spectral lines of a few milliAngstroms in width. On the other hand, spectroscopic studies of a dense plasma depend on the fact that when some atoms are part of such a plasma - which definitely is a system of interacting particles - their spectrum becomes changed. Types of "changes" which may occur in spectral line structure are alterations in the width of the line, in the wavelength position, in the intensity and in the line shape. These changes are dependent upon the state of the plasma, and may be used to determine densities and temperatures of the different constituent species.

This thesis deals with the broadening of atomic lines of the ArII and NII spectra in dense (electron densities near 10^{17} cm^{-3}) plasmas whose temperatures are a few electron-volts. The line broadening process has been variously described as "pressure" broadening because the breadth of a line shows a strong dependence on the density of the plasma, as "Stark" broadening because it is the electric fields of the perturbers that affect the atomic levels of the emitter, and as "collisional" broadening because electronic collisions are the dominant broadening mechanism. All these names are valid descrip-

tions of some aspect of the problem.

The theory of Griem, Baranger, Kolb and Oertel(1962) has been used by Griem(1964) to calculate widths and shifts of ArII lines in dense plasmas. Since these publications, the calculations have been refined by several workers - to be mentioned in due course - but the overall formalism remains unchanged. This theory is especially useful in regards to its applicability to nonequilibrium plasmas; if the particular approach of Griem et al. is valid, the shift-to-width ratio of a spectral line can be used to determine the electron temperature(see eg. Burgess and Cooper,1965b). Although shift and width both have linear dependences on perturber density, they have dissimilar dependences on temperature; thus, shift-to-width should only depend on temperature. And so the great attraction to shift and width measurement in the diagnosis of plasmas like those studied here is that L.T.E.(see eg. Cooper, 1966) in the emitting species is not required. Only the electrons need to have reached thermal equilibrium.

The theory does not achieve great success in its quantitative predictions of shift and width of ArII lines. The widths even from the recent calculations (Cooper and Oertel, 1967) agree to no better than 20% with experiment in a significant number of the cases treated. For shifts, there is very little experimental evidence with which the latest theory (Griem, 1964) can be compared. The present experimental work has been undertaken to find some values of ArII widths and shifts, with

the hope that this will inspire attempts to improve the theory where deficient.

The need for especially measuring the shifts of lines in ionic spectra is clearly revealed in the existence of the "Plasma Polarisation Shift" idea (see eg. Cooper, 1966). This is an attempt at explaining blue shifts of ion lines (eg. ArII lines) that the above theory is not able to predict. The collisional theory regards collisions as distinct events but does discuss the effects of correlations among perturbing electrons. But this afterthought calculation of plasma polarisation shift assumes that the electrons produce a static Debye potential around the emitter ion. This Debye theory yields shifts of the same order of magnitude as the collisional theory, and it is not clear how, or if, the two effects are to be added. Thus experimental evidence should be valuable when one has to decide between theories.

The plasma source used in this experiment was a pulsed arc discharge, similar to that described by Durand(1963). It was employed by Neufeld(1966) in the measurement of the profiles of ArII lines. The present work extends and refines these measurements. First, observations were made at several axial positions in the discharge to show that the arc was uniform so that spatial unfolding was not required. Secondly, a standard electrodeless light source was set up in order to measure line shifts. Thirdly, measurements were made in a Argon and Nitrogen mixture thereby keeping the Argon dilute

enough to make self absorption negligible. Finally, some NII lines were also measured and compared with the results of Day(1965).

Chapter 2 of this thesis discusses qualitatively the various factors that cause spectral lines emitted by a plasma to be different from those emitted by isolated atoms. Such phenomena can be due either to perturbations of the energy levels of the individual emitters or to other effects (eg. Doppler). First, a synopsis of the theory that predicts the Stark broadening of ArII and NII lines is given. Then comes a discussion of the other effects which, in principle, can broaden a line but which are shown to be unimportant in our case.

Chapter 3 describes the methods by which the observed line profile may be corrected for the instrumental broadening to obtain the true profile emitted by the plasma. In the next chapter, number 4, comes a description of the equipment and the experimental technique. The results for ArII and NII lines are presented in chapter 5. Finally, in chapter 6, we summarize the work by criticizing the technique and by discussing some interesting physics that is revealed by the measurements.

CHAPTER 2 - THEORY OF LINE BROADENING

Since the days of its infancy, the theory of line broadening has travelled a great distance and, in the course, has achieved definite progress. It has gone from the ideas of classical oscillators to those of quantum mechanical systems, from time averages to correlation functions, from "interuption" to "impact" broadening, and so on. In its advance, it has acquired a list of recipes for different situations. Some of these recipes were easily obtained; other more recent ones required good insight into the quantum mechanical atom and therefore have taken some time to formulate. This thesis is concerned with checking such a recent theory: that of pressure broadening of ion lines in cool, dense plasmas.

Reviews of developements in this field (Margenau and Lewis, 1959; Traving, 1960; Breene, 1961) are available. The state of the theory especially in reference to plasma radiation is well set out elsewhere (Baranger, 1958; Griem, 1964; Cooper, 1966). In the present chapter a qualitative review is given of the theory of line broadening in a cool, dense plasma as it is applied to the ArII and NII spectra. Our interest is in a plasma composed principally of ions and electrons and we focus our attention on the electrostatic perturbation of an emitting ion by electrons and other ions in its neighbourhood. For perspective, the account of Stark broadening will be

followed by a review of other mechanisms that can perturb atomic energy levels. It will be shown that these mechanisms, along with the Doppler effect and self absorption, can be ignored in this experiment.

A) Stark Broadening by Ions and Electrons

We begin with the work of Griem et al.(1962) in which they attack the problem of broadening in the HeI spectrum. This work makes a significant step beyond the earlier theory of Hydrogenic emitters. Inasmuch as the ArII and NII spectra have well separated fine structure like that of HeI, the work of Griem and others provides a good base from which to develope the ArII and NII theories. The following paragraphs attempt to state the important ideas that characterize the theory of isolated line broadening.

The basic interaction between the emitting ion and the perturbing ions and electrons is the Stark interaction $V = \underline{d}.\underline{E}$, where $\underline{d}$ is the dipole moment of the emitter and $\underline{E}$ the electric field of the perturber. In the limiting case where we consider only ionic perturbers, it is permissible to envisage a nearly static field because ion-ion collision times are much longer tham all other times of interest. At the other extreme, for electronic perturbations one thinks of the emitter experiencing many collisions while completing an emission, and one adopts the "Impact" approximation. In

general, both effects occur in the spectra studied here. The present discussion delays the problem of combining the two effects until the end.

Considering a certain transition, it can be shown (see eg. Griem, 1964) that the spectrum (viz. the line profile) has for its Fourier Transform the autocorrelation function of the light amplitude. If one writes the formula for the power spectrum of the emitter-plus-perturber system and then takes the Fourier Transform, the problem becomes one of finding the matrix elements of the dipole operator between unperturbed states, and the time-evolution operators of the system. The character of the former is well known from the stationary theory of atomic theory (eg. Condon and Shortley, 1935) ; calculating them is a fairly standard procedure and we take them as known. It is the framing and manipulation of the latter that constitute the major difficulty in the line broadening calculation. In order to obtain solutions, it is necessary to make certain approximations. Foremost are the "Classical Path Approximation" which allows writing the separated Schrodinger equation for the emitter ion, the "Impact Approximation" which says that collisions are fast and distinct, (for use with electronic collisions) and the "Quasi-Static Approximation" which says that collisions are slow (for use in ionic collisions).

In the Classical Path Approximation the time-evolution operator is calculated by assuming that the perturbers act

as classical particles following hyperbolic trajectories. The time-dependent Schrodinger equation of the emitter-perturber system is assumed to have solutions of the form $\chi(t)\,\varphi(t)$, where $\chi(t)$ involves only the emitter coordinates and $\varphi(t)$ involves only the perturber coordinates. Thus, the Hamiltonian of the perturber contains only its kinetic energy and the Coulombic attraction to the stationary emitting ion. It is found that $\chi(t)$ satisfies a Schrodinger equation whose Hamiltonian is that of the unperturbed ion plus the average, $\int \varphi^*(t)\, V\, \varphi(t)\, d\underline{x}_{pert}$, of the interaction potential V over the perturber wavefunctions . At this point the calculation of the autocorrelation function already requires two different sums or averages. First, there is a summing of dipole and time-evolution operators matrix elements between states of the emitter. Second, the sum over the states of the perturber becomes a statistical average over the perturber's impact parameters and velocities.

The range of validity of the Classical Path Approximation for colliding particles may be determined by examining the conditions necessary for creating the illusion of a classical particle passing the emitter. The de Broglie wavelength of the colliding electron or ion must be much smaller than the important impact parameters. We have already mentioned that the perturbation is caused by the $\underline{d}.\underline{E}$ interaction which is a long range force; thus since the distant collisions are the major contributors to the perturbation, most collisions can be

described using the Classical Path Approximation. Another requirement for this approximation is that the colliding ion or electron must relinquish negligible energy during a collision. That is, we require that collider's energy be much greater than the energy spread corresponding to the separation of the upper level from the nearest interacting level.

It is now expedient to recognize the two mathematical limits that correspond to ion and electron broadening. In all cases, the autocorrelation of the emitter goes to zero for large times: the narrower the line, the longer the time required by the autocorrelation to go to zero. If the inverse line width (width in frequency units) is small compared with the time to complete a collision, as with the low velocity ions, we may make the "Quasi-Static" assumption that during an emission all ionic perturbers are at fixed postions. We obtain first a Stark pattern of lines with natural widths and then perform an average over all possible perturber configurations. This averaging is done after separately calculating the distribution of the ion electric field in some plasma kinetic model. The fine structure of the Ar^+ and N^+ emitters is well spaced so that one expects the above ionic field to split finely the components of a multiplet in the usual quadratic Stark fashion (see eg. Condon and Shortley, 1935). Our ion-broadened line has an asymmetric profile whose Stark parameters cannot be analytically predicted in general but whose width and shift are heavily dependent on perturber density.

If, as for electronic collisions, it takes the auto-correlation function many collision times to differ appreciably from its unperturbed value, then the "Impact Approximation" can be made. When the suitable approximations are made in finding the time-evolution operators involved, the resulting line is shifted and given a Lorentzian shape. Since it takes many statistically independent collisions to disturb the emitter significantly, it is only the average effect of collisions that matters. One thinks of the light as being emitted by an isolated ion whose Hamiltonian contains H_e , where H_e is a time- average contribution given by the net results of electron collisions during an emission.

The requirements of the "Impact Approximation" are imposed in solving an Interaction Picture equation for the time-evolution operators. For the equation to be solvable, there has to be a time interval Δs such that the distribution of electrons around the radiator is statistically independent of the distribution at a time Δs earlier. In other words, this time must be much greater than the electron correlation time ω_p^{-1} ; where ω_p is the plasma frequency. On the other hand, the mean interaction between emitter and perturber during this interval of time Δs must be small. Physically, Δs must be shorter than the time between strong collisions which is of the order of the inverse line width. These Impact requirements can be stated alternatively as: the line width in frequency units must be much smaller than the

plasma frequency and the approximation will be valid for those parts of the line profile whose frequency separations from the line centre are small compared with the inverse collision rate.

When the Interaction Picture equation has been solved, the autocorrelation requires knowing only matrix elements of the zero-order Hamiltonian and of the perturbation operator (which is now time-independent) between unperturbed states of the emitter. In finding the perturbation operator, one averages over perturber velocities and impact parameters. The range of integration of the impact parameter between "cut-offs" is a matter of importance (Cooper, 1966). The lower limit is set by the fact the only collisions to be treated by this theory are the weak ones; collisions ocurring inside this minimum impact parameter are estimated separately with a strong collision theory (Griem, 1964). The upper limit is usually about one Debye length.

Further simplification may be possible for the N^+ and Ar^+ emitters in the cases where there is negligible perturbation expected in the lower levels of the lines (Baranger, 1962). One then considers the time evolution of only the upper states involved in the transition of interest.

It sometimes happens that interacting ionic levels are quite close together for high principal quantum number. In such a case, inelastic collisions can occur easily and it turns out (Griem et al., 1962) that one should consider possible correlations among perturbing electrons. Griem and others

(1962) show that the criterion for deciding on the importance of correlations is whether the splitting between interacting levels is of the order of the plasma frequency. When it is, one has to go to a Hydrogenic theory in which the emitter levels with this splitting are degenerate in orbital quantum number . However the theory that will be checked in this work assumes that the Ar^+ and N^+ upper levels are indeed isolated, ie., the splitting between opposite parity levels is much greater than the spread corresponding to the plasma frequency, and so we get "isolated" lines.

The Classical Path assumption makes certain requirements in the treatment of the atomic system. Since electrons involved in de-exciting collisions (from the upper level to the lower level) gain energies equivalent to the plasma temperature, the Classical Path assumption requires that the weak, broadening, inelastic collisions be much more frequent than the de-exciting collisions. This is with the additional proviso that the separation between strongly interacting levels be much less than the average electron energy. Thus, the present treatment is valid only when the electrostatic splitting lies between certain upper and lower limits.

As already mentioned, it is found that when an isolated upper level is Impact broadened, a Lorentzian line shape results: the width of the line profile is given by the imaginary part of the matrix element of the time-averaged perturbation Hamiltonian in the state corresponding to the upper level, and

the shift of the line peak with respect to the position of the unperturbed line is given by the real part of the same matrix element.

It is obviously important to have the correct quantum mechanical description of the unperturbed emitter states. Use of an incorrect coupling scheme, for instance, will lead to wrong widths and shifts if all interacting states are not considered carefully. Here, the LS coupling scheme is employed. The various j-levels of a given term will be perturbed identically and thus all the lines in a corresponding multiplet will have the same width and shift. Use of LS wavefunctions in this calculation will restrict the application of the theory to the lower numbered multiplets of ArII and NII. Both Ar^+ (Minnhagen, 1963) and N^+ (Eriksson, 1958; Day, 1965) have higher levels described under other coupling schemes.

The electronic and ionic perturber effects are "folded" together using the following recipe: find the Stark splitting due to the ion field for the natural line, calculate the electronic broadening of the above Stark components, convolute the electron-broadened spectrum with the probability distribution of the ionic field.

In a wide range of Argon or Nitrogen plasma conditions, including ours, the electron impacts are the dominant broadening mechanism whereas ions produce $\leqslant$ 10% of the broadening (Griem, 1964). The asymmetry in line profiles expected from the ionic broadening will be difficult to observe.

Griem(1964) gives tables of the half halfwidth w, the shift-to-width ratio d/w, and the "Quasi-Static Ion Broadening Parameter" α (a measure of the amount of ion broadening to be expected) for the lower numbered multiplets in the ArII and NII spectra (multiplet numbering in the notation of Moore, 1959). These are given as functions of temperature and at an electron density of 10^{16} cm^{-3}, with the understanding that at a given temperature $\alpha \propto (n_e)^{\frac{1}{4}}$, $w \propto n_e$, and $d \propto n_e$, where n_e is the electron number density. Subsequent experimental work on ArII widths has indicated appreciable discrepancies between theoretical and measured values. Later calculations have been undertaken (Griem, 1966; Roberts, 1966; Cooper and Oertel,1967) but the results are not as extensive as Griem's(1964) in that widths only are given, and these for a few temperatures. Throughout this thesis we refer to the whole halfwidth,that is, the full width at half maximum, as h, and the half halfwidth as w. Thus w = .5h .

B) Other Broadening and Shifting Effects

In order to complete this discussion on line broadening, we mention other effects and discuss why they are insignificant in the plasmas studied in this work.

i) Resonance Broadening(Griem, 1964) : Two like atomic systems, one in an excited state and the other in the ground state, can

be coupled together through the interaction of their dipoles and this leads to the exchange of energy between the two. This constitutes broadening due to the radiating system being damped by the partner in the interaction. In the case of N^+ and Ar^+ ions, their Coulombic interaction is much stronger than the dipole-dipole interaction.

ii) van der Waals Broadening(Griem, 1964): This occurs when two dissimilar emitting systems engage in dipole-dipole interaction. Again, the Coulombic force keeps the Ar^+ or N^+ ions far enough apart that this effect is negligible. Day(1965) shows how to mathematically estimate the order of magnitude of van der Waals broadening for plasmas like the ones studied here.

iii) Natural Broadening(Heitler, 1954): This is the lower limit on the breadth of a spectral line, for even if all external influences are removed from an emitting ion, its own radiation field will react with it. The theory predicts a damping out of the emitting system with a damping constant proportional to the sum of the spontaneous transition probabilities of all the lines originating at either the upper or lower states of the transition in question. For the spectroscopic equipment used in the present experiment, the natural width of all lines is extremely small and completely negligible

iv) Doppler Broadening and Shifting(Griem, 1964): The Doppler

effect in spectral lines arises because of the shift in the frequency of the light owing to the motion of the emitter with respect to the observer. With the ionic emitters moving at random velocities, the observed line has a shape determined by the velocity distribution of the emitters. The amount of Doppler broadening is proportional to the square root of the plasma temperature. In our plasma source, the temperature is sufficiently low that the effect is negligible; neither is there sufficient gross plasma motion to produce significant Doppler shift(Neufeld, 1966).

v) Self Absorption(Cooper, 1966): A photon emitted from the centre of a finite plasma either can be absorbed before escaping or it can escape. If the probability of escape is high, the plasma is said to be "optically thin", and conversely if the probability is low, it is said to be "optically thick". When a plasma is optically thick, photons emitted with a frequency near that of the line centre can become imprisoned whereas those in the tails can escape. This leads to a flattening of the line profile. Thus, when a "full width - half maximum" criterion is used to gauge line width, the line gets a greater width than it would in the optically thin plasma. It can be shown that the optical depths of the line centres in the plasma studied here may be large(Burgess and Cooper, 1965a). Thus care will have to be taken to arrange conditions so that even for the strongest lines self absorption is not important.

The effect of self absorption on line profiles is as follows: in an absorbing, homogeneous, L.T.E. plasma whose dimension along the line of sight is ℓ , the ratio of the intensity, $I(\omega)$, of a line whose absorption coefficient is $k(\omega)$ to that emitted in the optically thin case, $\epsilon(\omega)\ell$, is

$$\frac{I(\omega)}{\epsilon(\omega)\ell} = \frac{1 - \exp(-k(\omega)\ell)}{k(\omega)\ell} = \frac{1 - \exp(-\tau(\omega))}{\tau(\omega)} \quad (2.1)$$

Here the optical depth $\tau(\omega)$ may be found by assuming that emission and absorption are as in a black body cavity. Then(Griem, 1964)

$$\tau(\omega) = 2\pi^2 r_o c f_{mn} n_m \left\{1 - \exp\left(-\frac{\hbar\omega_o}{kT}\right)\right\} L(\omega)\ell \quad (2.2)$$

where $L(\omega)$ is the normalized line shape in inverse frequency units and all the other symbols have their usual significance.

From equation (2.1), it is seen that the true unabsorbed line shape in $\epsilon(\omega)$ is changed by a correction factor(the extreme right side) that is a function offrequency. To estimate the effect of absorption on halfwidths, one may assume for Impact broadening the emission and absorption lines have Lorentzian shapes with the same halfwidth. One then finds from equation (2.1) that the ratio $\frac{\delta}{W}$ of the observed halfwidth of an absorbed line to its true halfwidth is

$$\frac{\delta}{W} = \left[\frac{\tau_o}{\ln\left\{\frac{2}{1 + \exp(-\tau_o)}\right\}} - 1\right]^{\frac{1}{2}} . \quad (2.3)$$

τ_o is the optical depth at line centre.

The ratio $\frac{\delta}{W}$ is an increasing function of τ_o ;

it rises to 1.10 at $\tau_0 = 0.40$. Thus, if self absorption is tolerable only when $\frac{\delta}{W} \leqslant 110\%$, one must be sure to have the optical depth less than 0.40 for the centre of every line measured. Ideally, in the event of absorption, one might correct halfwidths using formula (2.3). In the present experiment, however, uncertainties in the oscillator strengths f_{mn} , in the population densities of the lower states n_m , and in the line shapes $L(\omega)$ would tend to produce large systematic errors in the measured halfwidths. The best approach is to make n_m as low as possible while maintaining the electron density, and therefore the true halfwidth, constant.

CHAPTER 3 - THEORY OF THE MEASURING PROCESS

The preceding chapter was a description of the intrinsic character of the spectral lines emitted by a plasma. No mention was made of what effect the measuring technique can have on a line profile in altering it from its true shape into some observed shape. The present chapter will give the general rules for removing (more technically: deconvolving) the instrumental effects from the observed line profile to get the true profile.

If a spectral line emitted by a plasma has an intensity profile $S_E(\omega)$, and if this light goes through a measuring process whose normalised response function is $S_A(\omega)$ and becomes $S(\omega)$, then we can say in all generality that

$$S(\omega_0) = \int_{-\infty}^{\infty} S_A(\omega_0 - \omega)\, S_E(\omega)\, d\omega \qquad (3.1)$$

where $\int_{-\infty}^{\infty} S_A(x)dx = 1$

S is called the convolution of S_A and S_E (see eg. Wiese, 1965). This convolution is valid when the functions being "folded" are statistically independent. There is no reason to expect any of the functions of interest here to violate this.

In many experimental situations, the problem of deconvolving S_A from S is not easily solved. However, let us mention two cases in which the unfolding can be done. First suppose that we had an apparatus with infinite resolving power

and an infinite range of output linear with respect to the input signal. Then we could close the chapter forthwith because the observed line shape would exactly duplicate the true shape. In reference to equation (3.1), this would mean replacing S_A by a delta function and identifying S and S_E. Such cannot be done in this experiment, however. Signals put through our spectroscopic equipment clearly suffer distortion.

Our basis for saying that S_A is not a delta function is that, when a very sharp spectral line is sent through our apparatus, it is broadened. Herein we come to the second of the two cases; mathematically,

$$S(\omega_0) = \int_{-\infty}^{\infty} S_A(\omega_0 - \omega)\, \delta(\omega)\, d\omega \quad . \qquad (3.2)$$

Physically this equation implies that if we send monochromatic light, whose spectrum is represented by $\delta(\omega)$, through the system we obtain the instrumental function S_A. This determination of S_A is the first step in our actual procedure. The second step is the placing of the now known S_A in equation (3.1) and then the unfolding of S_A from the known S, where S is the observed line profile when plasma light goes through the system.

S_A itself can be the convolution of two or more effects. In our case these include the broadening by the spectrograph itself, by the optics of the projection system in the comparator that scanned the plates, and by non-

linearities in the microdensitometer electronics associated with the comparator. The expected combined broadening would be difficult to calculate with sufficient precision (see Unsöld, 1938). A much better approach, alluded to earlier, is to send a very sharp spectral line through the whole system and empirically determine S_A . The latter technique is used in the present work.

The unfolding process is greatly simplified if S and S_A are recognizable as certain analytical functions called Voigt profiles. Equation (3.1) is the definition of the Voigt profile when S_A is a Gaussian profile and S_E is a Lorentzian, or vice versa. Further, as shown in van de Hulst and Reesinck(1947), S is a Voigt profile when S_A and S_E are also Voigt profiles. The advantage of using Voigt analysis is that analytical solutions of the deconvolution integrals can be obtained: tables of the entire range of possible Voigt profiles exist(van de Hulst and Reesinck, 1947). In the general case, when either S or S_A are not Voigt profiles, one must return to equation (3.1) either to devise a new analytical deconvolution or an approximate numerical solution.

According to the theory outlined in Chapter 2, one expects the plasma line profile S_E to be mainly Lorentzian, electrons being the dominant broadeners. But for the instrumental function S_A , as already shown, all one does is determine S_A as detailed in paragraph 4 of this chapter, hopefully to find that it has a Voigt shape to a good

approximation.

To demonstrate the basic properties of the Voigt functions one uses Fourier Transforms, The F.T. of equation (3.1) reads:

$$\tilde{S}(t) = \tilde{S}_E(t)\,\tilde{S}_A(t) \tag{3.3}$$

So if $S_E(\omega)$ is a Gaussian,

$$S_E(\omega) = C_E \exp\left(-\frac{\omega^2}{\beta_2^2}\right) \quad ; \quad \tilde{S}_E(t) = C_E' \exp\left(-\frac{\beta_2^2 t^2}{4}\right) \tag{3.4}$$

and if $S_A(\omega)$ is a Lorentzian,

$$S_A(\omega) = \frac{C_A}{1 + \left(\frac{\omega_0 - \omega}{\beta_1}\right)^2} \quad ; \quad \tilde{S}_A(t) = C_A' \exp\left(-\beta_1 t\right) \; . \tag{3.5}$$

With (3.4) and (3.5) in (3.3), one has

$$\tilde{S}(t) = A \exp\left(-\beta_1 t - \frac{\beta_2^2 t^2}{4}\right) \; . \tag{3.6}$$

It follows in the case where $S_E(\omega)$ and $S_A(\omega)$ are Voigt profiles that they both have transforms of the form in (3.6) , namely

$$\tilde{S}_A(t) = D \exp\left(-\beta_1' t - \frac{\beta_2'^2 t^2}{4}\right) \tag{3.7}$$

$$\tilde{S}_E(t) = E \exp\left(-\beta_1'' t - \frac{\beta_2''^2 t^2}{4}\right) \tag{3.8}$$

so that now $\tilde{S}(t)$ will be the transform of a Voigt profile whose Gaussian halfwidth is

$$\beta_2 = \sqrt{\beta_2'^2 + \beta_2''^2} \tag{3.9}$$

and whose Lorentzian halfwidth is

$$\beta_1 = \beta_1' + \beta_1'' \; . \tag{3.10}$$

Deconvolution of our apparatus profile $S_A(\omega)$ from our observed profile $S(\omega)$ is accomplished by the following simple procedure. Using the tables of van de Hulst and Reesinck(1947) we find the best Voigt fits for the two profiles. Then β_1 and β_2 characterize the observed profile $S(\omega)$ while β_1' and β_2' characterize the apparatus profile $S_A(\omega)$. The operations implied in equations (3.9) and (3.10) are then performed to obtain β_1'' and β_2'' characterizing the true profile $S_E(\omega)$. From the tables, one can find the width of the profile whose parameters are β_1'' and β_2'' .

CHAPTER 4 - APPARATUS AND TECHNIQUE

In this chapter the reader will find a description of all the apparatus that was used in exposing, calibrating and measuring the spectrographic plates for width and shift of lines. The chapter also deals with measurement procedure involving the Grant precision comparator and the subsequent computer processing of data.

Figure 1 shows the layout of the equipment used in obtaining spectrographic plates from which the width and shift of plasma lines were obtained. The specifications of each unit in Figure 1 are found in sections i) to v) of part A). Section vi) gives the method for finding the densities of the neutral density step filter that is needed for the intensity calibration of the plates. Part B) details the technique of setting up the equipment and exposing the plates. Following this, parts C) and D) respectively outline the remaining steps of the measurement on the comparator and describe how the data are reduced.

A) Spectral Line Sources and Spectroscopic Equipment

i) Energy Bank and Discharge Tube: It has been shown (Durand, 1963) that when an open-ended delay line, or the approximation to it known as the lumped-parameter delay line, is

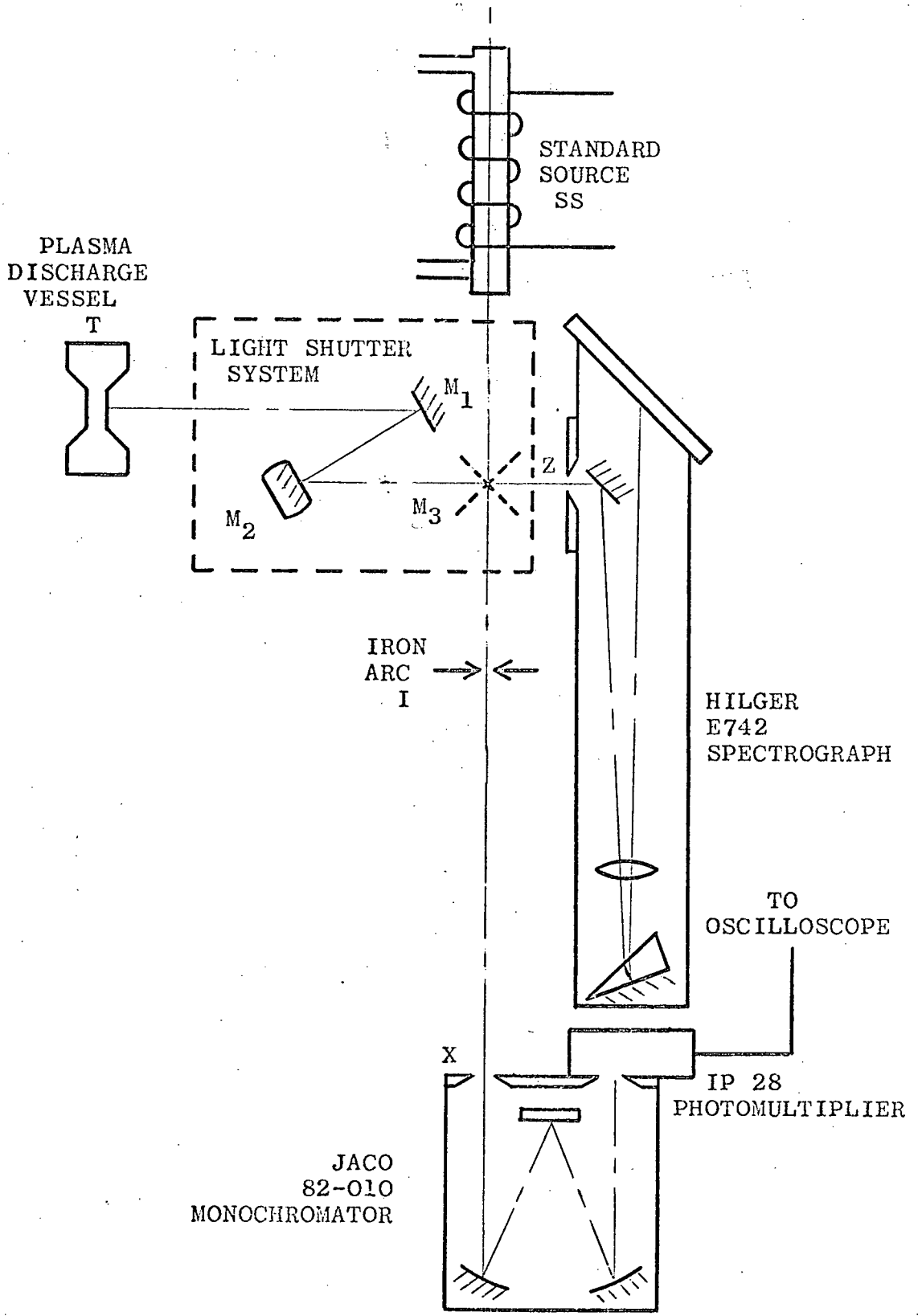

FIGURE 1

LAYOUT OF BASIC APPARATUS

charged up and then short-circuited through its characteristic impedance, the current flowing out is a square pulse. The height and duration of the pulse depend on the charging voltage and on the values of the inductances and capacitances constituting the delay line. A lumped-parameter delay line, symbolized in Figure 2 by what is inside the broken line, was constructed with the view that if a steady current could be made to flow for an appreciable time through a plasma, one might obtain a good approximation to a homogeneous, equilibrium plasma, that is, a plasma in which the temperature and the densities are well defined

The practical bank circuit was constructed of 5μf capacitors (CDE type NG 201) and 5μh inductances. Each inductance was a four turn coil of about 10 cm diameter, made by winding 1/4 inch copper tubing on a lucite form. The conventional open air spark gap switch S had two brass electrodes contained in a cylindrical housing of brass and lucite. An insulated firing pin sat in the ground side of the gap so that when a fast, high voltage pulse from a Theophanis(1960) trigger circuit was put onto it, the main discharge was initiated.

When the discharge current flowed through the plasma vessel T, the latter had a resistance of the order of milliohms, whereas the delay line characteristic impedance was about 0.5 ohms. Therefore, a specially constructed resistor R, of 0.5 ohms and able to carry kiloamps of current, was placed

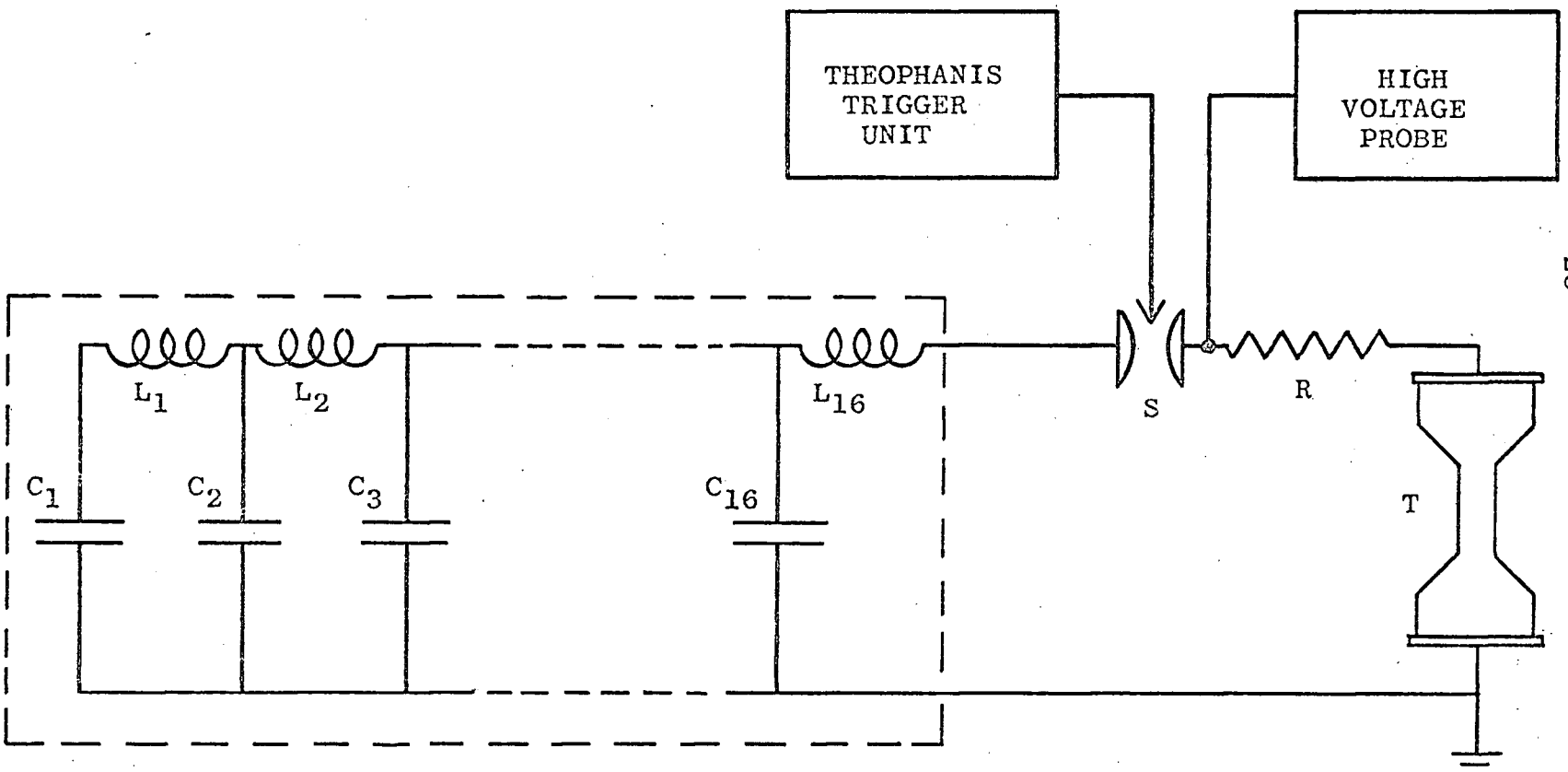

FIGURE 2

PLASMA DISCHARGE CIRCUIT

in the circuit as shown. The resistor (see Neufeld, 1966) had two copper surfaces of about 50cm by 10 cm immersed in a 10% solution of copper sulphate in distilled water. These electrodes were separated by 10 cm.

The plasma vessel, shown in Figure 3, was similar to the one employed by Durand(1963). Essentially, it was a piece of glass tubing with flared ends into which annular Aluminum electrodes had been sealed. The windows on the outside ends of the glass tubing in the centre of the electrodes facilitated end-on observations of the discharge. End-on observations were not made in this work, but the annular shape of the electrodes was essential to the production of the arc. This vessel was connected to a vacuum system via a tube running from a hole in the ground-side electrode. In the vacuum system, the pressure was measured by an aneroid gauge for the range 1 to 20 torr, or by a Pirani gauge for the 1 to 100 mtorr range.

ii) The Standard Source: An electrodeless discharge source of line radiation(Minnhagen, 1964) was built in order to provide the unshifted, very narrow lines required for the determination of the instrumental broadening function, as mentioned in chapter 3, and also to give the unshifted position of the plasma lines under study. Figure 4 schematically shows the vacuum system and electric circuit arrangements.

The gas for study was bled into the discharge tube D by a needle valve and removed by a diffusion pump through the Nitrogen cold trap. During operation, the gas was flushed

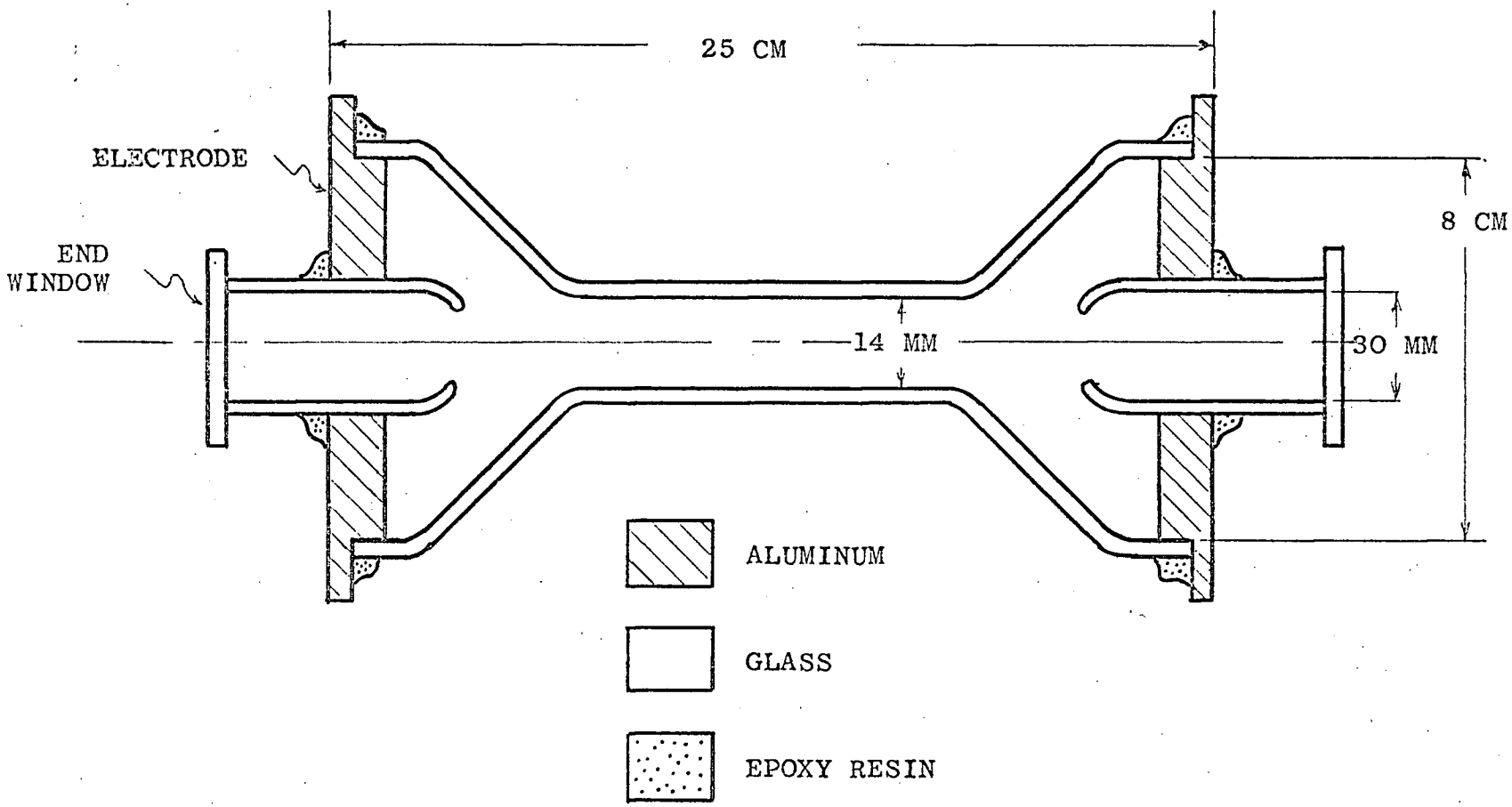

FIGURE 3

PLASMA VESSEL

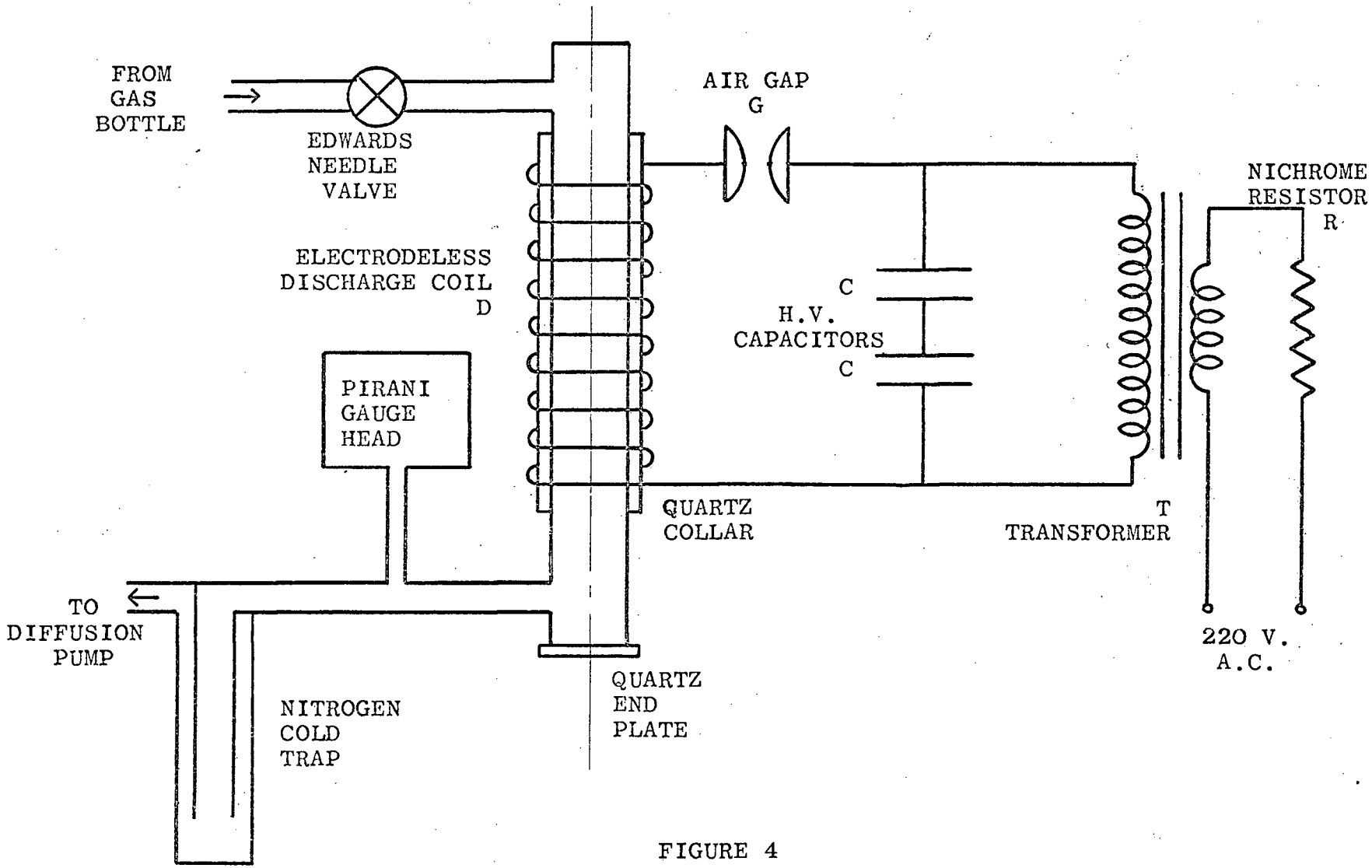

FIGURE 4

ELECTRODELESS STANDARD SOURCE

continuously through the system, its pressure being measured at the Pirani gauge head.

On the right side of Figure 4 is shown the electric circuitry which produced high frequency currents through the coil at D. Currents of about 20 amps flowed in the primary side of the transformer T, whose turns ratio was of the order of 1000 : 1. This primary current was limited by the 12 ohm resistor R′ which was made of appropriate lengths of 12 gauge Nichrome wire. The high voltage from the secondary charged two radar capacitors C (CDE type 52). Whenever the capacitors had a high enough voltage, the gap G broke down and underdamped oscillations occured in the discharge coil at D. The voltages at D were high enough to cause break down across the tube and thereby puncture the tube walls. To prevent this, a quartz collar separated the tube from the coil. The gap G had air forced across it in order to insure that it turned on and shut off cleanly for each rf burst. In order to allow different excitations in the tube, that is, to thus make possible a range of temperatures of the source, the gap distance was adjustable. Also the gas temperature could be varied to some extent by changing the pressure: the spectra of higher ionized species would appear as the pressure was lowered.

The radio frequency (~7MHz) resulting in the discharge was determined by the total capacitance C/2 (~ 0.0012μf) and by the inductance of the coil D. The latter was an eight-turn coil with a diameter of 5 cm and a length of 25 cm.

However, there was no requirement for tuning the oscillating circuit - a wide range of circuit components could produce an electrodeless discharge. The main requirement was that the rate of change of current in the coil be great enough to give the spectrum of interest.

iii) The Spectrograph: The photographic plates were all exposed in a Hilger E742 large glass prism spectrograph. This instrument had a Littrow mounted prism and a collimating lens of diameter = 7.5 cm and focal length = 170 cm. Reciprocal dispersions for typical wavelengths studied here (4100Å to 5500Å) lay in the range 5 to 14 Å/mm, and the resolving power was about 10^4. The normal slit width of 20μ was always used for exposing lines to be scanned ; when the step filter pattern was to be exposed, the slit was opened up to 90μ. The length of the slit exposed, on the other hand, was varied from 2 to 18 mm. A sliding cover on the Hilger F1386 slit produced the various lengths. A 2 mm length centred on the optical axis, and therefore on the slit centre, could be arranged as could two similar lengths starting from 1 mm on each side of the optical axis. In addition to these set apertures, a crescent-shaped opening could produce all lengths from 5 mm to 18 mm centred at the optical axis.

Kodak IF plates were used throughout the work. The use of I plates was dictated by the need for a fairly fast emulsion so that many plasma firings need not be taken even for

the weaker lines being considered. One aimed for as few shots per plate as possible in order to minimize the effects of drift in plasma conditions from shot to shot. The spectral range of 4100Å to 5500Å was best studied using the F sensitivity, although IO plates could just as well have been used in the blue end of the range.

Two devices were built to replace the plate holder and so fulfil special requirements in the setting up of the equipment. First, there was an adapter constructed which allowed an IP 28 photomultiplier assembly to be mounted in place of the plate. With this apparatus one could monitor the light coming to the plate area of the spectrograph and thus check the synchronization of the rotating mirror shutter, as described in part B). The photomultiplier had the usual cathode follower circuit to match its output impedance to the input impedance of the cable carrying the signal to an oscilloscope. Second, an incandescent lamp holder was also constructed to replace the plate holder. This lamp shone light from the plate region back through the optics, and was used in this way to align the whole optical system from the plasma discharge tube to the plate holder.

A very important attachment for the spectrograph was the neutral density step filter, Hilger number F1273. This comprised a quartz window onto which had been evaporated a 2 mm by 12 mm Rhodium neutral density filter of six steps, each step 2 mm long. The quartz plate was mounted in a barrel

which, in turn, could be fastened right in front of the spectrograph slit, with the length of the pattern lying along the length of the slit. The purpose of the filter was to attenuate to six different known degrees the intensity of a uniform light beam falling on the slit, so that the experimenter could obtain an intensity versus density curve (ie., the "H and D" relation) for the emulsion being exposed. The calibration of the intensity factors is described in section vi) of this part of the chapter, while that of the actual use of the filter comes in part B).

iv) The Monochromator: Figure 1 shows that the light from the discharge can be deflected from the spectrograph Z by the proper mirror at M_3 causing it rather to go to the monochromator entrance slit X. This JACO 0.5 metre instrument, number 82-010, was an Ebert mount type with adjustable entrance and exit slits. The monochromator was operated in first order where, for a 10μ entrance slit, the instrumental half-width was about 0.2Å; the reciprocal dispersion for wavelengths considered was 16Å/mm.

The light output from the monochromator was measured by an RCA IP 28 photomultiplier equipped with a cathode follower circuit for impedance match. Signals were taken via a 50 ohm cable to a multi trace oscilloscope for display, and could be used to check the temporal developement of a line intensity during an arc discharge. In the case where two line intensities were being compared, one had to use an exit slit

wide enough to allow the whole line profile to fall on the photomultiplier (because the data thus obtained was to be used in a theory that demands integrated line intensities, not peak values). For typical plasma line halfwidths, an exit slit width of 200μ was required.

v) The Light Shutter System: We include in this discussion of the light shutter all the optical elements between the discharge and the slit of the spectrograph. In addition, it will be necessary to describe here the function of the various electronic units which provided or verified synchronization of events during a discharge.

Rotating mirrors are widely used. In this experiment, the purpose of the system was to initiate the firing of the discharge, commence the plate exposure τ_D seconds after the discharge and continue to expose for τ seconds. Here, both τ_D and τ were required to be of the order of tens of microseconds. Mechanically these requirements could be stated as: the rotating mirror had to start sweeping an image of the interesting part of the discharge across the spectrograph slit τ_D seconds after the discharge started and to finish this sweep at ($\tau_D + \tau$) seconds after the initiation.

Figure 5 is a plan view of all the devices in the shutter system. The light from the plasma travelled in a horizontal plane defined by the axis of the discharge tube and the centre of the spectrograph slit S_2. The basic optical units were

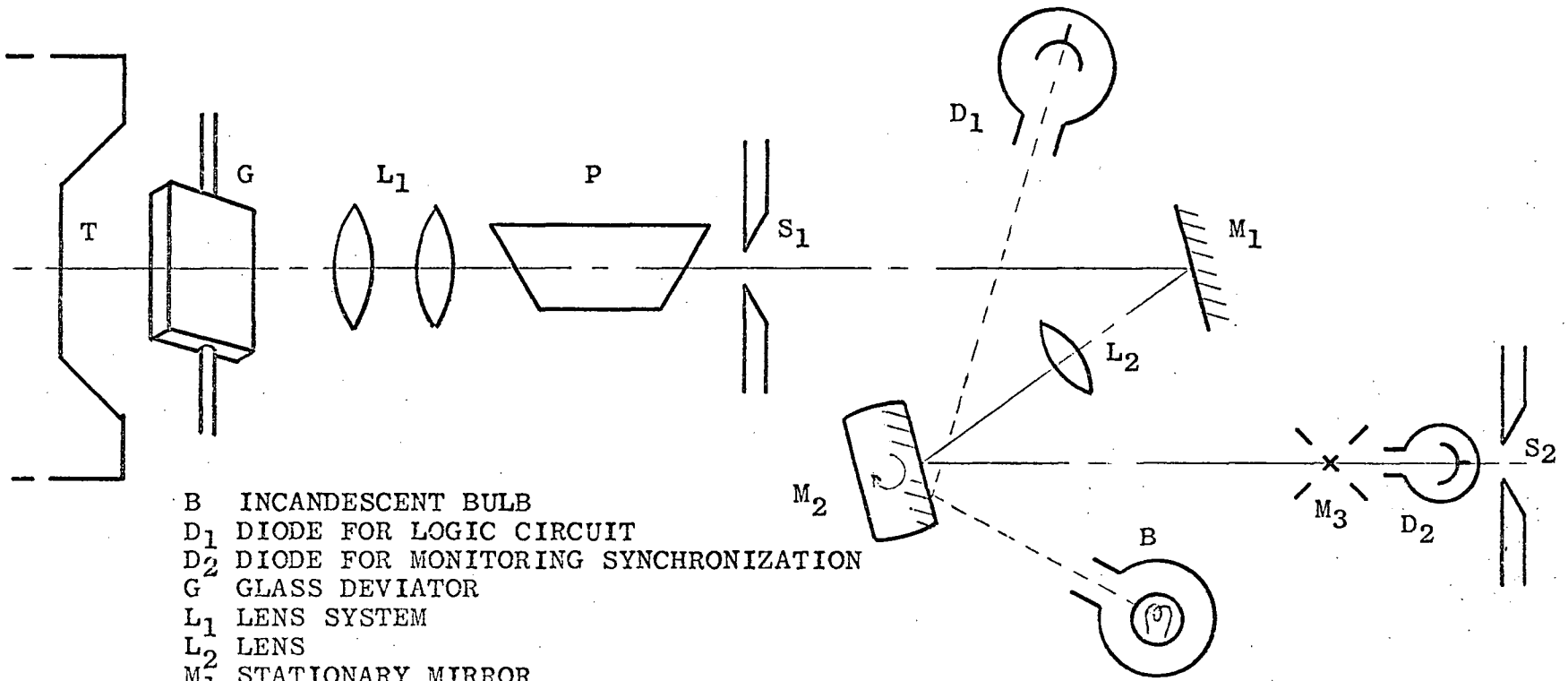

B INCANDESCENT BULB
D_1 DIODE FOR LOGIC CIRCUIT
D_2 DIODE FOR MONITORING SYNCHRONIZATION
G GLASS DEVIATOR
L_1 LENS SYSTEM
L_2 LENS
M_1 STATIONARY MIRROR
M_2 ROTATING MIRROR
M_3 REMOVABLE MIRRORS
P DOVE PRISM
S_1 SLIT
S_2 SPECTROGRAPH ENTRANCE SLIT
T PLASMA DISCHARGE VESSEL

FIGURE 5

SYSTEM FOR GATHERING AND SHUTTERING PLASMA LIGHT

lens system L_1, slit S_1, lens L_2 and slit S_2. Disregarding all the other elements in the set-up, one can say that the function of the first three just mentioned was to gather light from a small volume of plasma at T and focus it at S_2. Lenses L_1 took the plasma light and focussed it on S_1 ; S_1 was adjustable in width and thus limited the smallest dimension of the plasma volume sampled, namely, the dimension parallel to the tube radius. L_2 then focussed the image of S_1 onto S_2 .

Whereas the optics determined the width of the pattern swept across S_2, the length of the pattern exposed was simply limited by the sliding aperture immediately in front of S_2 which has already been discussed . The dimensions of the plasma volume sampled were small compared with those of the discharge : the sampled height was 0.5 mm, the width 2 mm, and the length equal to the distance on the optical axis through the discharge column.

One of the experimental aims was to see if there were any spatial inhomogenieties in the plasma and to correct the line profiles accordingly if such existed. It was desirable that the image of S_1 formed by the lenses L_1 at the plasma be horizontal so as to keep the radial dimension of the volume sampled as small as possible. This was accomplished by means of a Dove prism which rotated the image of S_1 by 90°. (It was judged that this would be a lot easier than setting the discharge tube vertical). G was a glass plate hinged on an axis parallel to that of the tube and it acted as a beam

deviator. The light was deviated by simple refraction in the plate; the plate's variable inclination meant that plasma volumes at different distances from the tube axis could be focussed at S_1.

The rotating mirror was the centre of the shutter system. Distances S_1 to M_1 to M_2, and M_2 to S_2 were determined from the speed at which the plasma image had to sweep across S_2, by the range of speeds available in the electric motor driving M_2 , and by the available space. M_1 was a 5 cm square front-silvered mirror; M_2 was similar and was driven by a 10,000 rpm Bodine motor, type NSE-13. The broken lines at M_3 show the positions of various mirrors inserted at times to direct other light beams to the spectrograph or to direct plasma light to the monochromator. In Figure 5 we show other items required for synchronization. Light from the tungsten lamp B was reflected off a lower part of rotating mirror M_2 and registered at photodiode D_1. This lamp-diode combination created a voltage signal telling the logic circuitry that the mirror M_2 was in position. The lower part of M_2 was used so that this light when reflected would pass below S_2 and D_2 at the time when M_2 was sending it in their direction. D_2 was placed directly in the plasma light path but below the portion that entered the spectrograph. D_2 monitored the arrival of the plasma light during a plate exposure run.

Figure 5 is not to scale; the specifications of the final

set-up were:

Distance	T to L_1	20 cm
"	L_1 to S_1	45 cm
"	S_1 to M_1	30 cm
"	M_1 to L_2	11 cm
"	L_2 to M_2	10 cm
"	M_2 to S_2	27 cm
Width of slit	S_1	1 mm
"	S_2	20 μ

The lining up of the whole optical system has already been referred to; incandescent light was shone into the back of the spectrograph and then through the shutter ensemble with the rotating mirror clamped so that the light reached the tube. Thus the "inverse" image at the tube showed the cross-section to be sampled, and the different components, such as the deviator G, could be adjusted so that radiation was collected from the desired radial position on the discharge.

The circuitry employed to switch on the discharge is shown in Figure 6 . Neufeld(1966) describes in ample detail the sequence of events during a discharge and only a condensed account need be given here. A pulse of a few volts was created by sweeping the light from the trigger lamp across the photodiode D_1. This pulse was inverted and shaped by a Schmidt trigger; it then triggered a Tektronix units 162 and 163 combination that put out a pulse of 5 volts delayed with respect to the shaped pulse by a time τ_t . These two pulses were summed in a coincidence unit that produced a 25 volt pulse when the

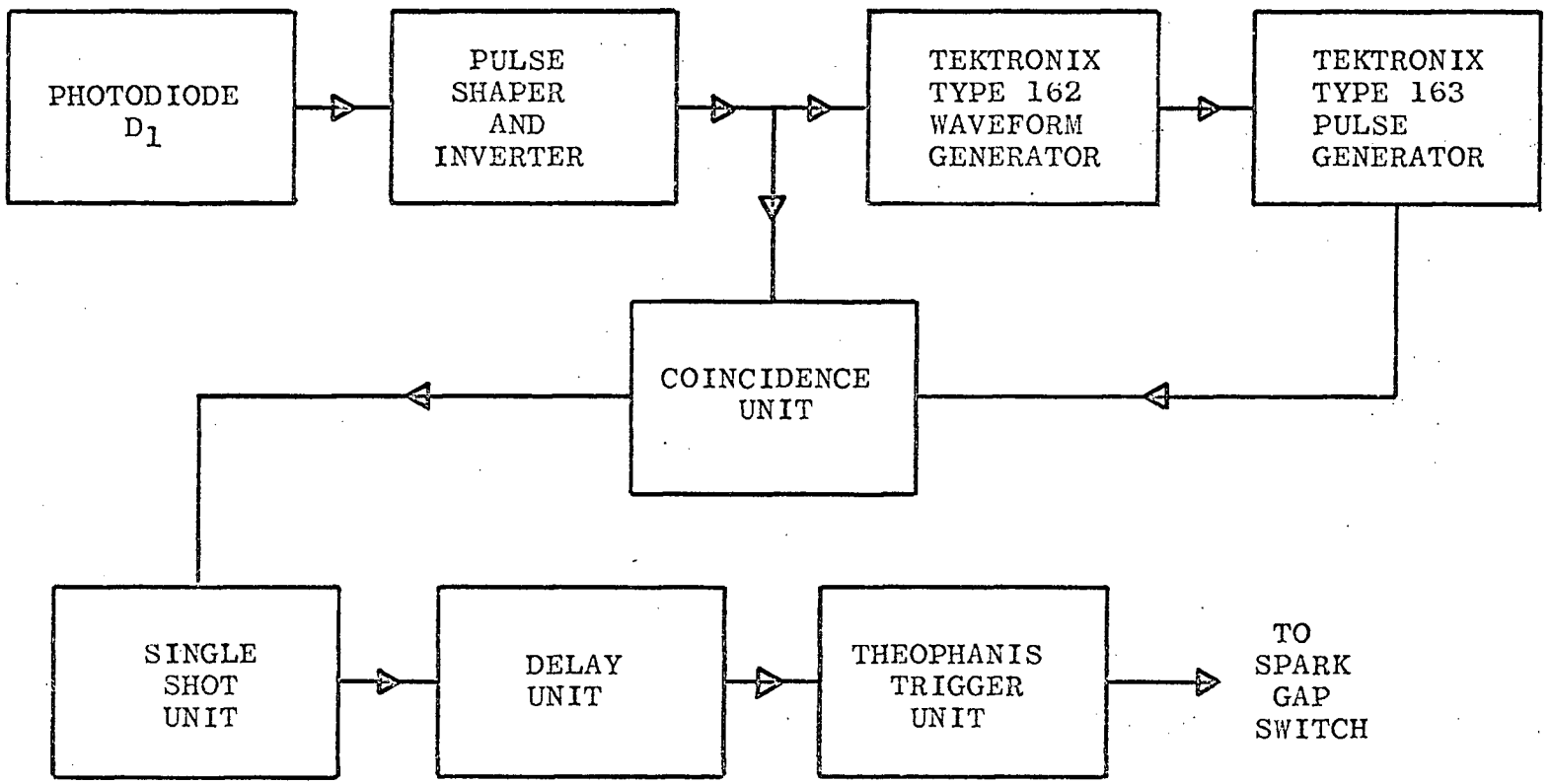

FIGURE 6

LOGIC CIRCUIT FOR SHUTTER

two input signals arrived together. Thus, when M_2 had been accelerated to a frequency of $(\tau_t)^{-1}$, the coincidence circuit put out a 25 volt pulse which caused the single shot unit (a bistable multivibrator) to trigger the delay unit. This unit had a continuous range of delays from 1 μsec. to 1000 μsec. After the set delay, the unit emitted a sharp, positive, 25 volt pulse that triggered the Theophanis circuit which then initiated the pulsed-arc discharge.

The time τ_t was set in advance knowing the following: the mirror would be sweeping an image of S_1 past S_2 for τ seconds. The given values of τ and the distances S_1-M_1-M_2 and M_2-S_2 determined the frequency of rotation of M_2 at which the bank had to fire. Also, the delay unit had to be adjusted to provide the correct τ_D (the time between bank discharge and the start of the exposure). Let us suppose that the rotating mirror had just reached firing frequency. Then, when the tungsten bulb image hit D_1, the coincidence circuit put out a command to fire. At firing frequency, the time between the creation of this coincidence pulse and when the plasma light started to sweep across S_2 was, say, τ_s. Then the delay unit would be set to give a delay of $(\tau_S-\tau_D)$.

At τ_t after the first exposure, the image of S_1 was again being swept past S_2. However, the plasma life-time was much smaller than τ_t, and therefore no "double exposure" problems arose.

D_2 shown in Figure 5 was a very small photodiode whose

junction was placed right in front of S_2 and just below the aperture that admitted plasma light. It sampled the light pattern as it passed the slit and so was useful, along with the photomultiplier unit on the spectrograph back, for establishing and monitoring the synchronization. Neither output was used in the synchronizing logic; they were displayed directly on an oscilloscope.

vi) Calibration of the Step Filter Densities: In section iii) a neutral density step filter was referred to as part of the basic equipment of the spectrograph. Figure 7 shows the apparatus employed to arrive at the "known" densities of each step of the filter. One used the standard technique of first establishing the linearity of the photomultiplier-recorder system and then measuring the relative transmissions of the steps. Linearity was proven by plotting the recorder output versus D^{-2}, assuming that the slit - ribbon lamp configuration was a point source, and without the filter in position as shown. In both the linearity check and the transmission measurement , the light chopper - photodiode - phase sensitive detector combination was employed in the usual way to reduce the photomultiplier noise at the output. With 200 μ slits in the monochromator, the relative transmissions of the six steps were obtained at 200Å intervals over the spectral range of 4000Å to 5600Å.

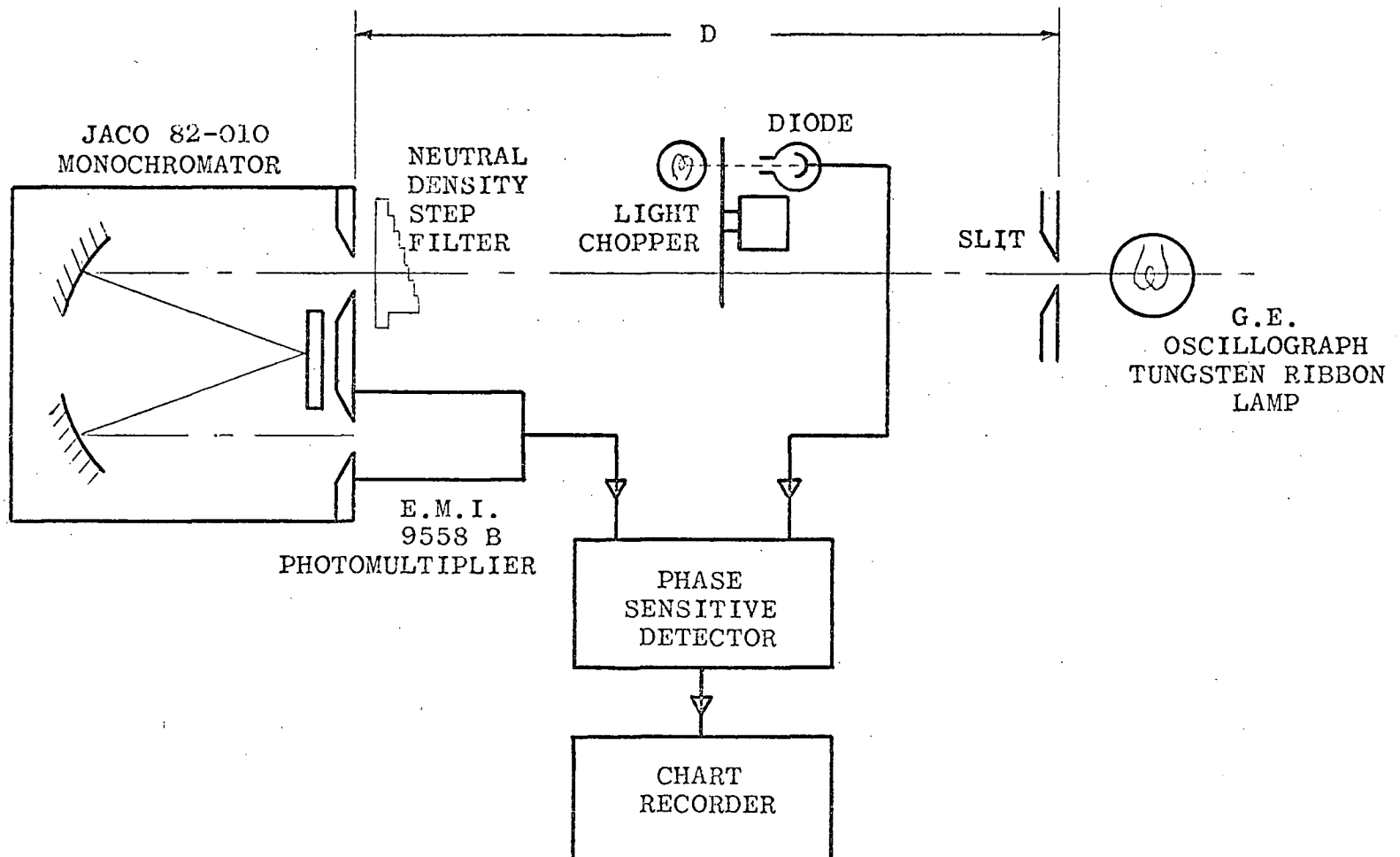

FIGURE 7

APPARATUS FOR STEP FILTER CALIBRATION

B) Plate Exposure Technique

In this part, we outline how the equipment described in part A) was used to obtain photographic plates on which width and shift of spectral lines could be measured. Included here are the study of time-resolved intensities of typical lines, the method of firing the delay-line bank for plasma line photography, the superposition of standard lines from the electrodeless source and finally, the development. This part follows the sequence of operations of a typical experiment.

i) Line Identification and Calibration: The gas to be studied was bled through the standard source, Figure 4, and the appropriate mirror was placed at M_3 in Figure 1 to reflect light from the standard source into the spectrograph. Photographs of the standard source were then taken with a 2 mm by 20 μ slit. M_3 was changed to reflect light from the iron arc I into the spectrograph whose aperture allowed the iron arc spectrum to straddle the electrodeless spectrum as recorded on the plate. For the iron arc photograph, one used the two 2 mm by 20 μ slits centred at 3 mm from the optical axis on both sides of the standard spectrum.

The above plate could be used to identify the lines that the electrodeless discharge was producing. The conditions of excitation and the length of exposure were varied and the photographic process repeated until satisfactory plates of

the desired spectrum (ArII or NII) were obtained.

Next, a choice was made as to which range of the spectrum for study was the most interesting and yet could be photograhed on one plate. This wavelength range was selected to contain measurable lines from a variety of multiplets and with a variety in shift and width. With this spectral range and a 2 mm by 20 μ entrance slit, one photographed the electrodeless discharge of the gas of interest. Then, another portion of the same plate was exposed to the same source through the step filter and using an 18 mm by 90 μ slit. This plate was used to calibrate the spectrograph for the reciprocal dispersion and the instrumental broadening function.

ii) Establishing the Shutter Timing: The intensity-versus-time graphs for a few of the lines chosen for shift and width measurement were obtained. Referring to Figure 1, M_2 was clamped to reflect the image of S_1 via the appropriate mirror M_3 to the monochromator slit X. The whole system was lined up by shining laser light back through the system to the tube. Next, with the IP 28 photomultiplier on the monochromator, the plasma tube was discharged by manual triggering of the Theophanis unit. On a dual beam oscilloscope, both the discharge current form and the photomultiplier output were displayed versus time. The times τ_D and τ were easily read from these oscillographs (Typical oscillographs and the criteria for chosing τ_D and τ are given in the next chapter).

iii) Exposing the Plate: Having adjusted the circuitry to give the correct delays and exposure, one checked the timing by firing the bank and monitoring the discharge current waveform, the output of D_2, and the voltage from the photomultiplier on the back of the spectrograph. The delay unit time was changed until the photomultiplier pulse occurred at the correct time with respect to the start of the discharge. Furthermore, the lateral position of D_2 could be adjusted mechanically until the pulse from it during a bank firing coincided with the pulse from the photomultiplier. Thus, although the photomultiplier for the spectrograph back was not in operation during a plate exposure run, the diode D_2 could verify synchronization on all plasma discharges.

The exposure routine will now be described with reference to Figure 8, In this Figure are shown all the necessary images of one spectral line. The long dimensions of the images are the same as those of the slits producing them because our spectrograph had a magnification of 1. The plasma was discharged using the shutter synchronization for as many times as were required to obtain correctly exposed plasma line images, a 2 mm by 20 μ slit being used. The resulting broad, shifted line image is shown as the plasma line in position B. Then the plate was exposed to the standard source with the two off-centre 2mm by 20 μ slits. Resulting standard lines are shown straddling the plasma line in positions A and C. Next, the spectral range setting of the spectrograph was changed - for

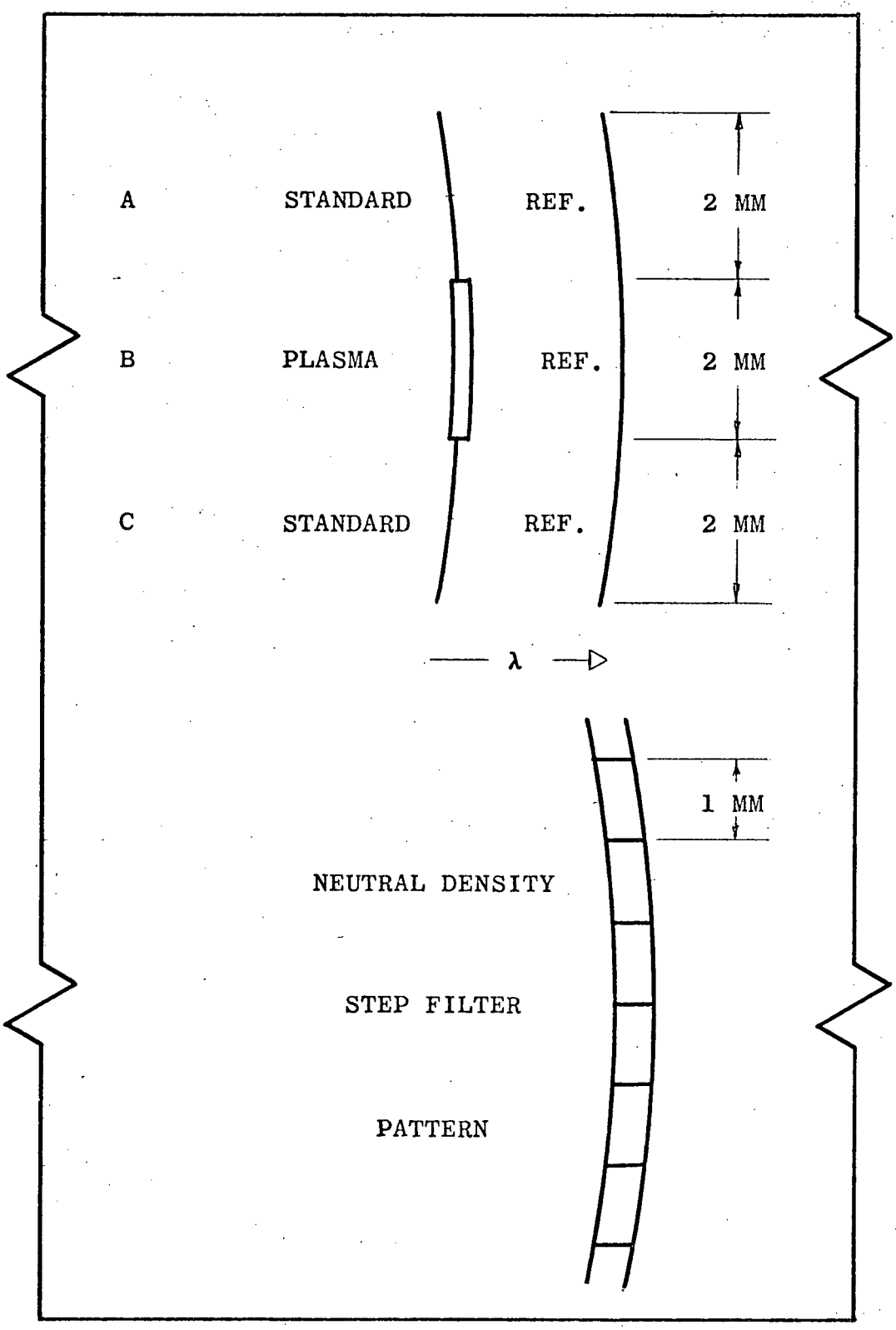

FIGURE 8

PORTION OF A PLATE WITH ALL NECESSARY IMAGES OF ONE LINE

some plates it was raised, for some, lowered - by about 10Å and the slit dimensions changed to 6 mm by 20 μ, centred on the optical axis. The plate was exposed to the standard source for the same length of time as the "straddling" spectrum; thus the 6 mm long reference line was produced (in Figure 8 the spectral range was lowered). Finally, the plate was lowered with respect to the spectrograph to expose a new part of it, and the standard source again photographed, this time with the step filter covering a 18 mm by 90 μ slit. The exposure time again was that given the straddling spectrum and the resulting step pattern image was centred at 15 mm below B on the plate.

In practice, one could put two A-B-C patterns, corresponding to two different positions for viewing the discharge, on the same plate along with one step filter pattern. The second A-B-C pattern was placed on a different vertical position of the plate. In Figure 8 it would be placed above the A-B-C pattern shown.

Whether the spectrograph's spectral range was raised or lowered for the reference line depended on the relative density of other lines near the one to be studied. For instance, the shift to lower range in Figure 8 would be recommended if there were a greater density of lines on the blue side of the line than on the red side

In the exposing of a plate as just described, care had to be exercised to obtain measurable plates. In reference to

the H - D curve (see eg. Mees and James, 1966) as sketched in Figure 9 below, one knew that the film blackening (ie., the density) for our plates did not depend linearly on the time-integrated intensity of the light incident on it. In particular, it was possible to saturate a line image if it received too great an exposure (region S in Figure 9). Useful line images were those whose blackest filter step had a density well below complete saturation and whose line peak similarly had a density on the straightest part of the H-D curve. In Figure 9, A to B is the best range. Optimally this was true for the plasma, standard and reference lines; since no two lines in the study had exactly the same intensity and since the ratios of line intensities in the plasma were different from their ratios in the standard source, a number of plates with different combinations of exposure times for the two sources were needed to get correctly exposed plates for all the lines in the group studied.

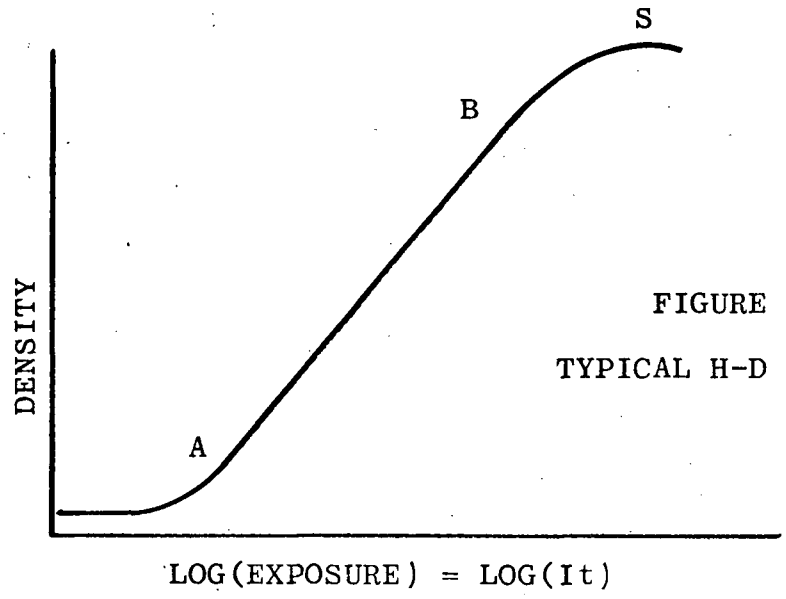

FIGURE 9

TYPICAL H-D CURVE

It was not obvious that one could use the intensity calibration curve produced from the electrodeless discharge light and apply it to the plasma line profile because reciprocity or intermittency failure might obtain(see Mees and James, 1966). However, it was found after some trial experimentation that it was much quicker and more convenient to achieve a uniform illumination of the 18 mm long slit by the electrodeless source than by the plasma source. Therefore, in order to justify this use of the standard source, step filter patterns were photographed on the same plate using both sources. With similar densities on the two patterns, relative intensity - versus - microdensitometer transmission curves read on the precision comparator (description to follow) agreed to well within the total error in the intensity calibration method. Having thus confirmed that there were no such photographic failures, one used the standard source for all step filter patterns without further check.

iv) Plate Development: Development of the Kodak IF plates was done essentially as prescribed by the manual (Kodak,1962). In order to minimize adjacency effects which occur especially in the sharp, standard line images , the plate emulsions were brushed continuously with a camel hair brush during development. In addition, after the regular two hour wash, the plates were rinsed in distilled water to remove residual dirt.

C) Measurement of Plates on the Comparator

i) The Comparator: The plates were scanned on a Grant Spectrum Line Measuring Comparator. In this apparatus, the plate stage was driven past a microdensitometer that measured the transmission of a small area of the plate. The longitudinal position of the stage could be measured differentially to $\pm$ 1 μ, while the transmission readings had a maximum range of 1 to 999 in integral steps. The actual end-points of the transmission scale were set for each plate to assure use of most of the scale: 980 for the unexposed part of the plate and 10 for zero transmission, that is, total blackening.

Tomkins and Fred(1951) describe the optical principles involved in the comparator. Essentially, for the transmission readings, a zoom lens system projected an image of a portion of the plate onto a slit in front of a photomultiplier. The magnification of the image was variable between 5 and 20, while the slit dimensions were variable in length from 1 mm to 25 mm and in width from 0.1 mm to 1.0 mm. Since lines were scanned across the width, the instrumental breadth therefore had limits of 5 μ and 200 μ.

The transmission reading and the stage position were continuously monitored by a Datex CDS - 1 system. This unit, in turn, was connected to an IBM 526 card punch for which the Datex instrument digitized the transmission and position readings. At each position on the plate where one required a

reading, the data were recorded by pushing a button.

Tomkins and Fred(1951) show that a comparator can be equipped to indicate approximately what the line profile looks like and which position on the profile is being viewed by the microdensitometer. In the Grant comparator, an image of the line was swept back and forth across a slit - photomultiplier combination identical to the one that measured transmission. The instantaneous signal from this photomuliplier was displayed on an oscilloscope screen where the horizontal sweep was synchronized with the motion of the line image. This image was exactly parfocal with that projected onto the transmission photomultiplier. When the image was centred on the transmission slit, the oscilloscope displayed two line profiles. These moved together as the line centre approached the slit centre. If the line was symmetrical, the two oscilloscope traces completely merged when the photomultiplier viewed the centre of the profile; only the peaks merged when an asymmetrical line was centred. In either case, one could readily determine which part of the line profile was being sampled by examining the oscilloscope display.

ii) Comparator Adjustment and Measuring Technique: Let us suppose that a line like that shown in the plate segment of Figure 8 was to be measured for shift and width. One first had to choose the best settings of magnifying power and transmission slit dimensions . The magnification and slit width

had to be set so that a small width of the plate was viewed and yet so that the transmission would still be close to 100% for the clear part of the plate. It was best to scan the plate with as small an instrument broadening as possible because the smaller that width in comparison with the observed width, the more reliable the deconvolution process. In fact, it was found that with narrow slits (less than 0.1 mm in width) it was impossible to get a suitably long range of transmission values. Thus the sensitivity of the transmission reading put a lower limit on the slit width.

After the magnification was set, the transmission slit length had to be adjusted to read as much of the line length as possible without encountering appreciable curvature in the image (see later in this section). But one wanted a long slit in order to average the transmission reading over as many emulsion grains as possible. Again one came to the requirement that there be enough light coming through the slit to ensure good transmission sensitivity. So then, the three parameters were interdependent and some experimenting was done before the optimal settings were found for the spectrographic plates at hand.

The procedure for measuring a plasma line for its width and shift is now given with reference to Figure 8. The position of the plate with respect to the stage was adjusted so that the central part of the reference line B was at right angles to the direction of travel of the stage. When the transmission

slit dimensions and the magnification had been set, (these were 0.5 mm by 10 mm and 12 respectively for all the work done here) and when the microdensitometer head had been zeroed correctly, the transmissions of the steps of the neutral density filter pattern were read.

At this point, the use of the reference line becomes obvious. In one uninterrupted sweep the standard and reference lines of position A were scanned. The drive was toward increasing wavelengths to avoid backlash problems in the stage mechanism. Likewise the pairs of images in positions B and C were scanned together. The distance standard-to-reference in position A could be checked against that in position C to verify that the plate had been correctly oriented on the stage and that there had been no disorientation of the reference line with respect to the plasma and standard lines at the time during exposure when the spectral range of the spectrograph was changed. Having found that these two distances in positions A and C agreed, one could subtract from their average the distance plasma-to-reference in position B. This difference was the net plasma line shift. All the distances referred to in the present discussion are between line peaks.

In this routine, the transmission and stage position data recorded during the scanning of the plasma B line constituted the data for the observed line profile. Usually, about 50 readings per plasma line scan were recorded; there was a greater separation between adjacent readings on a wide plasma

line than on a narrow one. The plasma line was scanned far enough out into the wings to ascertain how much, if any, correction would be required for continuum radiation. Standard and reference lines were always read with 5 μ intervals.

Curvature of line images is a well known phenomenon and readily observed on the plates taken in the Hilger E742 spectrograph. Since one was interested in scanning line profiles with a finite length of microdensitometer slit - which had to sample off-axis parts of the spectrograph slit image - one wanted to know the order of magnitude of curvature in the spectrograph. Erfle(1924) treats the geometrical problem and finds a formula for the displacements of the extremities of a slit image. However, in the present work, the curvature of images could be found satisfactorily by measuring the peak positions of small segments of a standard line image. For example, with reference to Figure 8, this was done by choosing a slit length small in comparison with the 2 mm length of reference B and then using the oscilloscope display and the stage lateral feed to find the central positions of the off-axis extremities in positions A and C with respect to the position of the line in the middle of B.

The curvature measured for lines in spectrum position B in Figure 8 was small and it was possible to choose a slit length for which there was insignificant effect on measured plasma line profiles. The method of finding shifts in positions

A and C where curvature effects may be significant is designed to remove such effects from the measured quantities. This is explained as follows: although the profiles of the standard line in position A and the reference line in position A, say, were both distorted and shifted by curvature, their distortions and curvatures were identical. The distance between their peaks in position A was the same as what would have been measured between their peaks in position B if we had exposed the standard line there instead of the plasma line. This rests on the facts that

a) one set the stage drive perpendicular to the centre of the lines in position B; hence, the microdensitometer slit sampled exactly the same portion of the standard and reference images in position A, and

b) standard and reference lines had the same curvature because they were produced by the same wavelength of light.

D) Computation and Analysis

An IBM 7040 computer was used to change the line scan transmission data into relative intensities, to calculate some widths on the smoothed profile, and to find the centre of the profile. In what follows, we outline the basic methods used in the program to evaluate the required numbers.

First, the program took the transmission data for the different steps of the neutral density filter and, with the known relative intensity calibration, in effect created its own H-D curve. Then the line scan readings were translated into relative intensities by interpolation on this H-D plot. The whole profile was smoothed out by applying second degree polynomial least squares fitting to consecutive groups of five points. This part of the program was able to calculate the abscissa of the line peak after it had found the parabola best describing the five points on the profile closest to the peak. This value of line centre was printed out in the units in which the abscissae (stage positions) had been read, namely in microns.

After normalising the smoothed profile to one at the peak, the computer calculated some widths of the profile as follows: it found the two sets of three consecutive points on both shoulders of the profile which were closest to the 80% level, which we call $.8I_o$. It then performed quadratic interpolation to determine the abscissa of this $.8I_o$ ordinate, on both sides of the profile. Subtraction of one abscissa from the other gave the $.8I_o$ width. The $.7I_o$, $.6I_o$, ... $.1I_o$ widths were similarly found. All the widths were normalised to the $.5I_o$ width, which is the whole halfwidth, and the whole halfwidth and the six normalised widths were printed out, the former in microns.

The particular form in which the widths of an observed

line were printed out by the computer was chosen to facilitate the use of van de Hulst and Reesinck's(1947) tables from which the β_1 and β_2 characterizing the profile (see page 23) could be immediately found. This step was not done by the computer because some judgement was required to decide which β_1/β_2 best fitted the calculated widths. Having found that there were satisfactory Voigt fits for the plasma (observed) line, and the standard (apparatus profile) line, one performed the Voigt deconvolution for the width of the true profile. The half halfwidth and the shift of this line were converted from microns to Angstroms using the dispersion curve.

CHAPTER 5 - THE EXPERIMENT

A) The ArII Lines

i) The Conditions of Measurement: The plasma that was used to create ArII line radiation was produced by discharging the delay-line bank, charged to 13 kV, through a Nitrogen-Argon mixture at an initial pressure of 10 torr. The final results were taken from plates that had been exposed to plasma radiation during a 15 μsec interval centred in time at 20 μsec after the commencement of the bank current.

Some initial work was necessary to establish the feasibility of spectroscopic studies with this source and then to find the conditions, just stated, in which data was best gathered. Neufeld(1966) took side-on pictures of the discharge with a high speed Barr and Stroud framing camera. At some initial pressures ($\sim$ 100 mtorr) the plasma was constricted to a thin filament that moved unstably about the vessel. At the chosen pressure of operation, 10 torr, the vessel appeared uniformly illuminated over its diameter during the whole current pulse. The plasma stability thus guaranteed a suitably stationary source of radiation.

Spectra of the standard source were photographed for varying exposures and electrodeless discharge conditions. A gap of 19 mm in the secondary circuit and an Argon pressure

of 20 mtorr in the discharge tube led to a satisfactory standard spectrum, it being almost exclusively ArII lines. These were identified using Minnhagen's(1963) classification. With the identification complete, the line scan data taken from the same plates were used to plot the dispersion curve and the instrument broadening function of the spectrograph over the 4000Å to 5600Å range. The reciprocal dispersion is shown in Figure 10, in which the vertical errors are $\pm$ 0.1 Å/mm .

The apparatus broadening function was obtained as outlined in chapter 4. Approximately 70 line scans were processed in order to obtain the line profile as a function of wavelength. The shape of the instrument profile was constant across the spectral range. In terms of the normalised widths, it was:

Y	$.8I_o$	$.7I_o$	$.6I_o$	$.5I_o$	$.4I_o$	$.3I_o$	$.2I_o$
X	.544h	.696h	.846h	1.000h	1.179h	1.375h	1.588h

This constituted a good fit to the Voigt function for which $\beta_1/h = 0.225$. Therefore, in all the deconvolutions, one used the Voigt analysis with this particular Voigt function representing the instrumental effects. The instrumental whole halfwidth h is shown in Figure 11 as a function of wavelength. Here, the vertical errors are about $\pm$ 3 μ.

Next, the time-integrated spectrum of the plasma was photographed along with the standard source to allow the identification of the plasma lines. The plasma did emit a few

FIGURE 10

RECIPROCAL DISPERSION OF THE SPECTROGRAPH

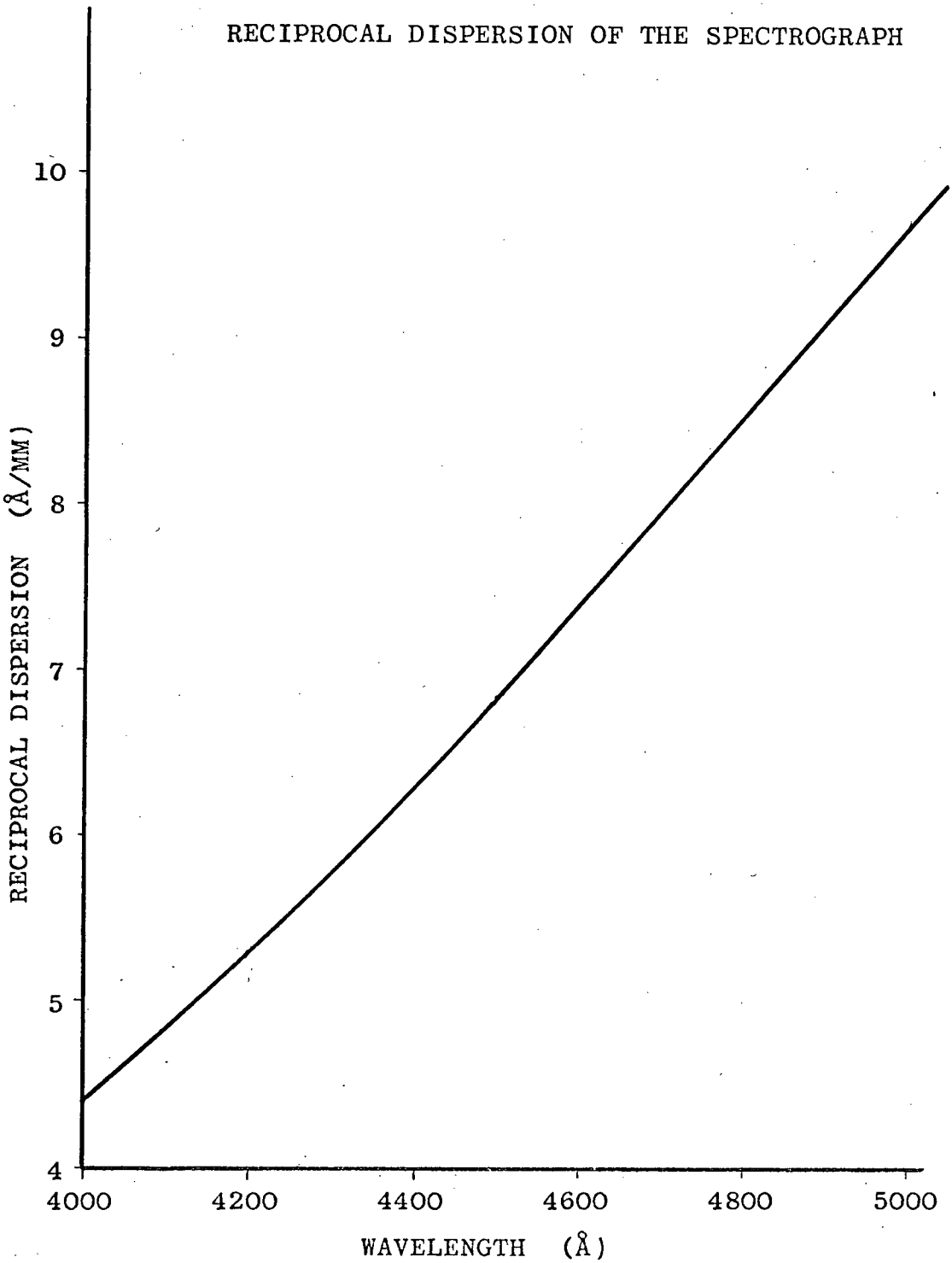

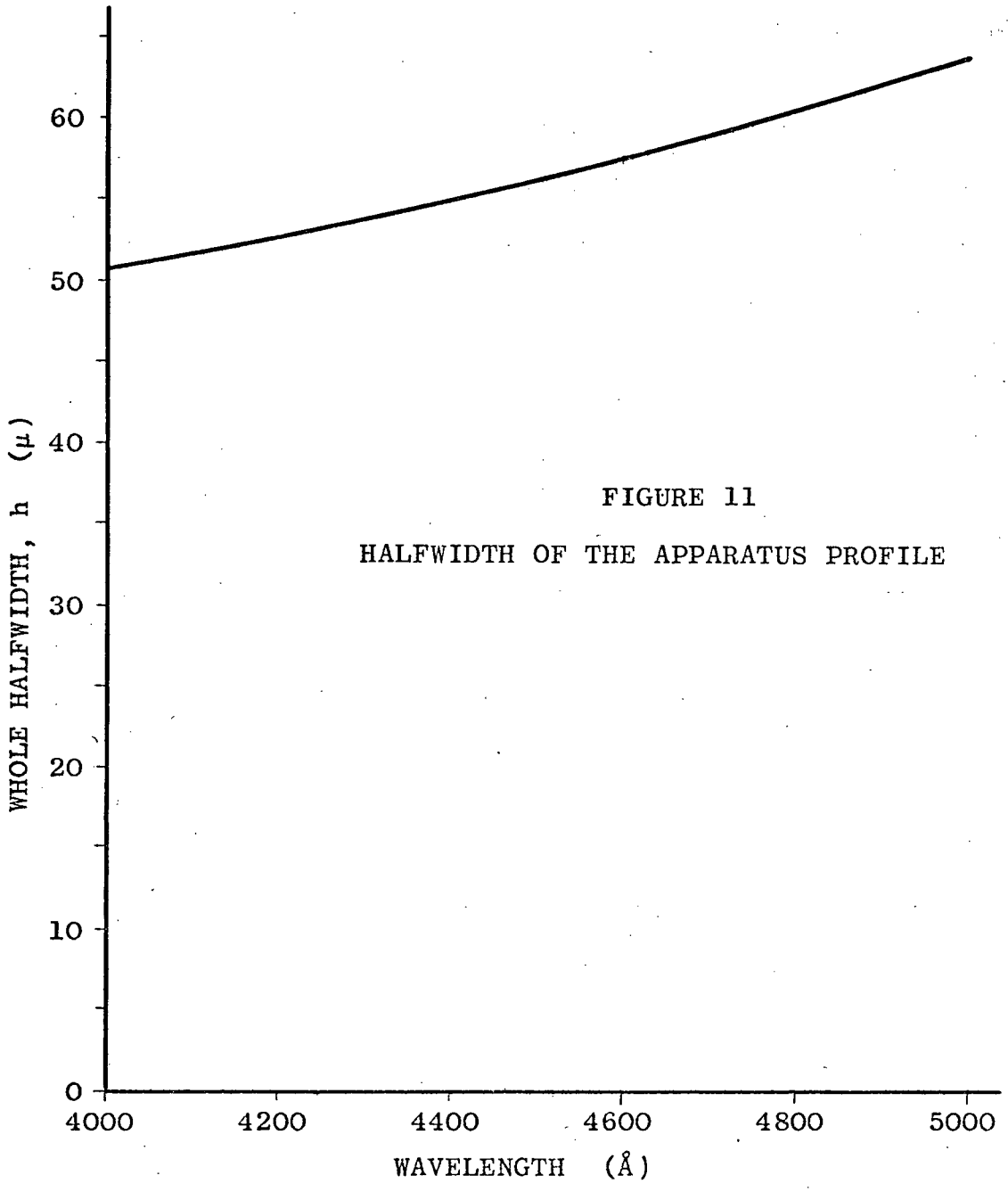

FIGURE 11

HALFWIDTH OF THE APPARATUS PROFILE

impurity lines, but ArII and NII lines dominated, no matter which dilution ratio of Nitrogen to Argon was used. Some ArII lines were not sufficiently removed from all others to allow study of their widths and shifts; this restriction was not serious since other lines in the same multiplet could be measured.

It was evident from the identification that the spectrograph with its glass optics would allow the interesting range of 3750Å to 5000Å to be photographed on one 10 inch plate. Lines in this region were selected for study. These lines were well spread out, represented a variety of multiplets, including the most intense ones(therefore the most commonly measured lines) , and had interesting diversities of shifts, widths and intensities.

Time-resolved studies were carried out with the monochromator for the lines: ArII 4014, ArII 4806, NII 3995, and NIII 4097. Each intensity-versus-time graph had the same shape during the times of interest , when both an on-axis and an off-axis portion of the discharge were viewed. During a 15 μsec period that started about 13 μsec after the onset of the bank discharge, the line intensities were maximal and varied by about 10%. Measurement of the NII 3995 and NIII 4097 signals permitted an estimate of the plasma temperature. ArIII 3795, a strong line in the spectrum of the twice ionized Argon atom, could not be detected above the background with the photomultiplier.

The intensity-versus-time relation for ArII 4806 was measured at four different radial positions on the discharge column. The results are shown below along with the bank current waveform,.

FIGURE 12

HISTORIES OF PULSED-ARC CURRENT AND A LINE INTENSITY

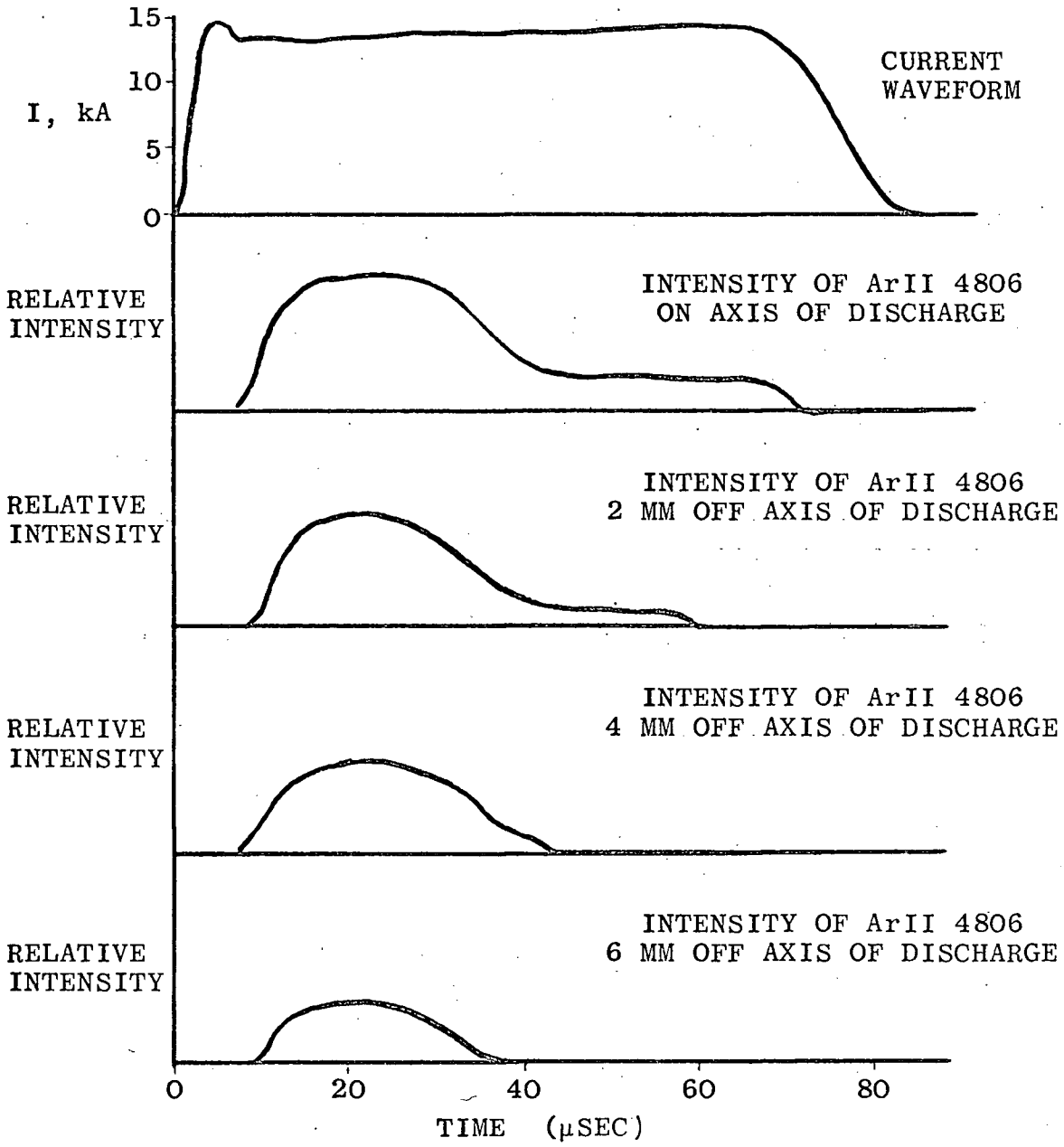

One wanted to expose the plates when the light output from the plasma was large and not changing much, it being assumed that when a line intensity was least changing was the most likely time to have thermal equilibrium. It was desirable that the line intensities be as high as possible during the exposure in order to minimize the number of plasma shots per plate. On the basis of these criteria and the foregoing oscillograms, the times τ and τ_D in the shutter synchronization were set so that the exposure time was the 15 μsec interval centred at 20 μsec after the onset of the bank current.

Considerable experimentation with the discharge conditions was required to obtain measurable plates of all the lines for the four radial positions on the arc given in Figure 12. A most important reason for this experimentation was the elimination of self absorption of lines. For this purpose, the Argon gas was diluted with Nitrogen in order to lower the density of Ar^+ ions and yet keep n_e high enough to produce wide, Impact broadened lines. It was found, for instance, that when pure Argon was discharged, ArII 4348, ArII 4806 and other strong lines could have optical depths between 1 and 10, when reasonable estimates were made for the density of Ar^+ ions and for the temperature, and in which Olsen's(1963) transition probabilities were used.

The amount of dilution of Argon by Nitrogen was chosen to be just high enough to avoid self absorption, At the same time, the number of plasma shots per plate had to be as large

as was necessary to yield usefully exposed line images. Excessively high dilution was avoided because then the experimenter would have to take more time in procuring well exposed plates and would rely more heavily on the plasma reproducibility. To check that absorption was not occurring, one measured the widths and shifts of several lines with a representative range of intensities at a dilution ratio just above or just below the proposed conditions of study. It was found that the shifts remained the same for all dilution ratios and that therefore the electron density was also constant. The agreement between the widths of a line at two dilutions was thus taken to indicate that there was no self absorption of that line. The stronger ArII lines 4348 and 4806 had to be exposed at $p_o(N_2)$: $p_o(Ar)$ as 10 : 1, where p_o is the partial pressure of the gas in the tube prior to discharge. The majority of lines were taken in a 3 : 1 mixture, while the two weak lines, ArII 4132 and 4933, were observed in pure Argon. Between 5 and 10 shots per plate were required for all the lines.

On the most heavily exposed plates it was difficult to see any blackening in the plasma spectrum that could be attributed to continuum radiation. That is, the density between sufficiently separated lines, according to both the microdensitometer and the human eye, was negligibly different from the emulsion background fog seen on the unexposed portion of the plate. Our plates were exposed and developed so that the lines of interest had their $.2I_o$ points above the background

fog - below this, little could be said about the line shape. Since the photographic fog always masked any continuum blackening on the plates, no correction was made for continuum in the data reduction process.

Figure 13 shows two interesting parts of an actual ArII plate taken from a pure Argon discharge. These pictures show lines with a quite large range of intensities. Hence, the bright ones, like 4806, may be self absorbed and/or overexposed and not measurable on this plate. Nevertheless, one can see the relative widths of the standard and plasma lines, the cleanness of the spectrum, some plasma lines with large shifts and curvature (in the step filter pattern). The scale at the bottom is that produced by the spectrograph during the photographing; in order to show this scale conveniently in our picture, the plate is inverted compared with that in Figure 8.

ii) The Results: The results of measuring 19 ArII lines are shown in Table I. Having found widths and shifts at four radial positions on the discharge, one noted that none of the lines exhibited a systematic dependence of w or d on the distance of the viewing position from the tube axis. The average values are shown in this table in which the data are grouped according to the dilution ratio for which the lines were exposed.

The half halfwidths of the lines in Multiplet 6 - which is a favourite with theoreticians and experimentalists - were used in estimating the electron density of the plasmas. Griem's

FIGURE 13

TWO PARTS OF AN ArII PLATE

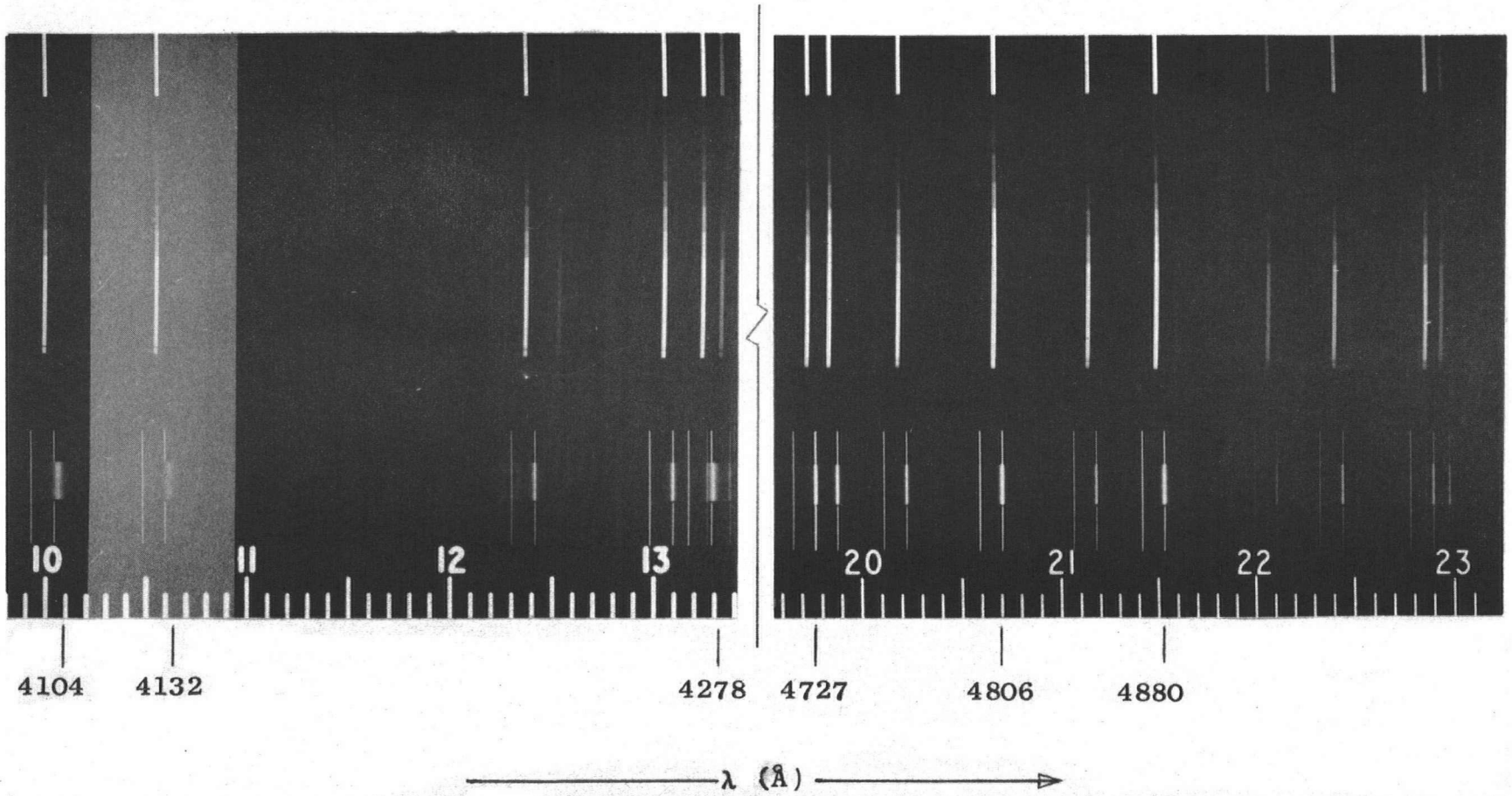

TABLE I

MEASURED ArII WIDTHS AND SHIFTS COMPARED WITH CURRENT THEORETICAL AND EXPERIMENTAL DATA

MULT. NO.	WAVE-LENGTH, Å	HALF HALFWIDTH w, Å			SHIFT d, Å	SHIFT-TO-WIDTH RATIO	
		THIS EXP.	ROBERTS (1966) EXP.	GRIEM(1966) THEORY	THIS EXP.	THIS EXP.	GRIEM(1964) THEORY
6	4806	0.49±.06	0.50±.07	0.31	-0.18±.04	-0.37	-0.07
7	4348	0.41±.04		0.29	-0.10±.02	-0.27	+1.01
		$n_e = (2.4 \pm .4) \times 10^{17} cm^{-3}$, kT = (2.6±.2) ev					
6	4736	0.48±.05		0.30	-0.18±.04	-0.38	-0.07
6	4848	0.48±.07		0.30	-0.22±.04	-0.46	-0.07
7	4267	0.39±.05	0.39±.06	0.28	-0.14±.03	-0.36	+1.01
7	4331	0.45±.04		0.28	-0.13±.03	-0.29	+1.01
7	4380	0.46±.05		0.28	-0.14±.04	-0.30	+1.01
14	4727	0.53±.04		0.37	-0.19±.03	-0.36	
14	4880	0.62±.05	0.57±.06	0.37	-0.19±.04	-0.31	
15	4658	0.54±.04			-0.15±.03	-0.28	
15	4765	0.54±.04			-0.16±.03	-0.30	
17	4579	0.53±.05			-0.06±.04	-0.11	
31	4590	0.55±.06			-0.08±.04	-0.15	
31	4610	0.54±.06			-0.11±.04	-0.20	
32	4278	1.07±.08			+0.30±.05	+0.26	
39	4482	0.55±.05			+0.05±.04	+0.09	
52	4104	1.27±.12			+1.03±.08	+0.81	
		$n_e = (2.3 \pm .4) \times 10^{17} cm^{-3}$, kT = (2.6±.2) ev					
6	4933	0.40±.05		0.25	-0.20±.05	-0.50	-0.07
32	4132	1.26±.12			+1.05±.07	+0.83	
		$n_e = (1.9 \pm .4) \times 10^{17} cm^{-3}$, kT = (2.6±.4) ev					

(1964) theoretical halfwidth was multiplied by a factor of 2.6 which Jalufka and others(1966) say is required to secure agreement with experiment in this multiplet. This corrected width was used to scale the observed widths to find the value of n_e. It was assumed in this calculation that Griem's values of width exhibit the correct temperature dependence in order to correct for the difference between Jalufka's temperature(1.6ev) and ours(Jalufka found w(Mult.6)=0.20Å at $n_e=1.03\times10^{17}cm^{-3}$).

The measurement of the intensity ratio of NII 3995 and NIII 4097 has been alluded to already. The resulting value, along with the electron density and the oscillator strengths for these lines given by Griem(1964) were substituted into the equilibrium relations (see eg., James, 1965) to find kT, the temperature connecting the population densities of the N^+ and N^{++} ions. This temperature had to be that guessed during the electron density estimate (at a given density, the line widths do have some temperature dependence). If it was not, the n_e and kT calculations were iterated until the intensity ratio observed, the width of the Multiplet 6 lines, n_e and kT were consistent.

The electron density and the plasma temperature thus found are shown in Table I. The errors on the temperatures are produced by the uncertainties in all the parameters of the Saha equation that was solved for kT, namely, in the theoretical line strengths, in the experimental intensity ratio and in the experimental electron density. The line strengths are

probably good to $\pm$ 25%, while the intensity ratio has significant error from the high background in the NIII 4097 intensity measurement and from possible self absorption effects in the NII 3995 intensity measurement. The error in n_e shown has contributions from the total error assessed in our experimental width determination - this will be discussed later in this thesis - and from the uncertainty that Jalufka et al. place on their scaling factor.

It is possible to write the equilibrium relations showing the intensity ratio I(ArII 4014) : I(ArIII 3795) as a function of electron density and plasma temperature. Using the oscillator strength for ArII 4014 quoted by Griem(1964) and the LS coupling formula with Bates and Damgaard's(1950) radial matrix elements for the ArIII 3795 oscillator strength, one found that the above ratio was 23:1 for the $p_o(N_2):p_o(Ar)$ as 3:1 plasma. This is consistent with the experimental results cited in the preceding section. During those measurements, a signal 1/23 of the size of the ArII 4014 signal at the photomultiplier would be buried in the background. Indeed, no ArIII 3795 light registered at the photomultiplier.

Table I shows the comparison with recent theoretical predictions and with the results of an experiment(Roberts, 1966) in which the temperature was very close to ours. One might also cite other experimental evidences for the widths, like that of Popenoe and Shumaker (1965), but they would not be as relevant because the temperatures there were significantly

lower than 2.6 ev. Similarly, there is other theoretical work on widths (Roberts, 1966; Cooper and Oertel, 1967) containing refinements on Griem's(1966) calculation but predicting values little different from Griem's. In Table I, Roberts' experimental widths have been scaled down by a factor of 2.3/ 4.4 - or 2.4/4.4, as the case may be - to convert from his n_e condition to ours. Likewise, the theoretical estimates in columns 5 and 8 are evaluated for the plasma conditions indicated. This work is among the first to measure ArII line shifts in dense plasmas, so there is little else available for comparison in the shift column except the work of Popenoe and Shumaker(1965) in which the width and shift of ArII 4806 seem to be well measured. They find that w = 0.36Å and d/w = -0.49 at n_e = 2.4×10^{17} cm^{-3} and kT = 1.1 ev . Their low temperature makes comparison somewhat strained, but the order of magnitude of the ratios of their numbers to the present ones is that predicted by the Impact theory. It is thus concluded that this one instance of shift measurement in ArII agrees with the author's result.

The only theoretical calculations of shift available are those of Griem(1964) and these are contained effectively in column 8. For all three multiplets studied commonly by Griem, Roberts and the present author, the two experimentalists measure the same widths and these disagree with the theoretical results. Also, the shift-to-width ratios measured bear little resemblance to the theory's predictions. However, the Impact

theory requirement that all lines from the same multiplet have the same width and shift is substantiated in the present work.

For the theoretical widths, the total uncertainty deriving both from the basic uncertainty in the calculation (containing, for instance, inaccurate wavefunctions) and from the stated errors in the n_e and kT values is almost large enough to allow one to say that the theory does agree with experiment. No such argument is possible in the case of the shift-to-width calculation: this quantity depends only on the temperature and one finds, for instance in Multiplet 6, that the error in the temperature maps into an error in d/w of about $\pm$ 0.05 .

B) The NII Lines

i) The Conditions of Measurement: This part of the experiment on NII radiation was undertaken to check the work of Day(1965), especially to see if the present photographic technique was better than the usual monochromator-photomultiplier approach for measuring widths and shifts. Day studied eight lines, namely: NII 3006, NII 3838, NII 4026, NII 4530, NII 4553, NII 4614, NII 5045, NII 5495. Of these, 3006 was not considered in the present work because the wavelength lay outside the spectral range of the existing apparatus.

The electrodeless discharge was run with Nitrogen at a

pressure of 1 mtorr and a secondary circuit gap of 19 mm. Molecular bands were much in evidence in the resulting spectrum, produced mostly in the N_2 and N_2^+ systems. Nevertheless, the standard source, also clearly produced the six lines of longest wavelength studied by Day. NII 3838 was present but obscured by a molecular band. The atomic lines were identified under Eriksson's(1958) classification.

It was found that a good plasma for studying the NII lines was the same as that from which most of the ArII data were obtained: a $p_o(N_2):p_o(Ar)$ as 3:1 mixture was discharged at a bank voltage of 13 kV and with a starting pressure of 10 torr. As in part A), the plates were exposed to plasma light for a 15 μsec interval starting at 13 μsec after the initiation of the discharge.

Time-integrated photographs of the N_2-Ar plasma spectrum did not show NII 3838 clearly. For this reason and also in view of its obscurity in the standard spectrum it was removed from the list of lines to be studied. This left the six lines of longest wavelength in Day's list, and they were all exposed on one spectral range setting of the spectrograph, 3950Å to 5500Å. Five lines from Multiplets 1 and 2 of the NIII spectrum had already been identified in the plasma spectrum. The use of one of the lines in Multiplet 2, NIII 4097, for the temperaure determination has been described in section i), part A) of this chapter.

The instrumental broadening function was taken to be

the same Voigt profile as found for the spectral range used for the ArII lines. The reciprocal dispersion curve, Figure 10, was extrapolated to give the value required for NII 5495; the instrumental halfwidth was obtained by treating the graph Figure 11 similarly. Then, the accuracy of the extrapolated values was checked by scanning some identified NII lines in the 5495Å region of the plate.

The variety in widths and intensities of the NII lines of interest led to the requirement of between 3 and 10 plasma shots per plate and a complementary range of exposure times of the standard source. Since none of the optics in the system was changed between the work described in part A) of this chapter and that in part B), the comparator measurement routine also required no adjustment. Again, there was no need to correct line profiles for underlying continuum radiation. All the NII lines in this experiment had Voigt profiles, none showing significant asymmetry. Among the deconvolved true profiles there was a variety of shapes but, again, the Lorentzian shape dominated.

ii) The Results: The widths and shifts of the six NII lines are shown in Table II. The values are the averages of readings taken from on-axis and from 3 mm off-axis of the discharge. Sampling only at two positions, instead of four as previously, was adopted after it was confirmed that, as with the ArII lines, the widths and shifts in NII showed no dependence on which part of the discharge was photographed. In this table,

TABLE II

MEASURED NII STARK PARAMETERS COMPARED WITH CURRENT THEORETICAL AND EXPERIMENTAL DATA

MULT. NO.	WAVE-LENGTH, Å	HALF HALFWIDTH w, Å				SHIFT-TO-WIDTH RATIO d/w			
		THIS EXP.	DAY (1965) EXP.	BERG (1967) EXP.	GRIEM (1966) THEORY	THIS EXP.	DAY (1965) EXP.	BERG (1967) EXP.	GRIEM (1964) THEORY
4	5045	0.63±.07	0.19±.03		0.37	+0.03±.03	+1.00±.34		+0.84
5	4614	0.58±.05	0.17±.03	0.46±.05	0.28	+0.21±.04	+1.10±.37		+0.87
29	5496	0.69±.17	0.22±.03		0.58	-0.29±.17	+0.83±.28		+0.67
40	4026	2.90±.45	1.58±.25		2.53	-0.03±.09	-0.09±.32		-0.22
58	4553	2.66±.28	0.55±.15	2.07±.21	0.94	-0.03±.12	-0.28±.56	0.0±.3	-0.58
59	4530	2.67±.70	1.84±.18	2.53±.25	3.22	-0.05±.13	-0.16±.20	-0.3±.2	-0.25
n_e, $10^{17} cm^{-3}$ →		2.3	2.3	2.3	2.3				
kT, ev →		2.6	1.6	1.93	1.6	2.6	1.6	1.93	2.6

the plasma conditions are those estimated for the ArII measurements at the same dilution ratio, and the errors indicated on the results of this experiment are the sum of random and systematic uncertainties as mentioned in part A) previous. Again, in almost all of the cases, the random error is significantly greater than the systematic.

One could expect the strong lines in our discharge to suffer self absorption. Using the estimates of n_e and kT already found for the ArII lines and assuming that for this 3 : 1 mixture

$$n_e = \frac{7}{6}n(N^+) = 7n(Ar^+),$$

where $n(N^+)$ is the number density of N^+ ions and similarly for the Ar^+ ions, then one could evaluate the optical depth according to equation (2.2). This was done for the lines in Multiplets 4, 5, 29, and 59 with Griem's(1964) oscillator strengths. The greatest reduction in width according to equation (2.3) was that of the 5045Å line - 7%. All other lines had 4% or less broadening due to self absorption. This correction was significantly less than the random error on the width and was not applied because the main interest in this NII work was to check shift-to-width ratios. In comparison with the random uncertainties in the values of w and d, the above self absorption correction was completely negligible.

A review of the literature revealed no published oscillator strengths for the lines in Multiplets 40 and 58. However, the two lines were observed to have intensities and

widths of the same order as the 4530Å line. Since this line was calculated to have little broadening by absorption, the former two were also assumed to be negligibly affected in this way.

Although the primary purpose of this work on NII was to photographically verify Day's(1965) results, of shift measurements, experimental and theoretical results from other sources are also given in Table II in order to indicate overall agreement. Since the publication of Day's results, Griem (1966) corrected the theory and pointed out that there was agreement between it and Day's numbers only to within a factor of 2. Roberts(1966), and Cooper and Oertel(1967) also amended the NII theory but found discrepancies comparing their predictions with the work of Day. Again, therefore, Griem's(1966) work has been taken as representative of the progress in the field of width calculation. As opposed to the case of the ArII widths, there is no independent experimental data on NII widths at the temperature of the plasma under study here. In Table II, the experimental values, and their errors, from Day(1965) and from Berg et al.(1967) have been scaled to correspond to the electron density found in the plasma of the present work.

The most relevant experimental reports on NII shifts are those of Day(1965) and Berg et al.(1967), while Griem's(1964) work is the latest theoretical effort for such lines. In order to simplify comparison, only the shift-to-width ratios are shown

in Table II; one thus avoids any apparent disagreement between theory and experiment arising from a poor n_e calibration.

The agreement among the ratios of the NII 4026, NII 4530, and NII 4553 lines is obviously superficial. These ratios are evidently too small to be measured by any of the three techniques; for all experiments, the percentage error in shift, and therefore in shift-to-width ratio, is of the order of 100%. For the three narrow lines NII 4614, NII 5045, and NII 5496, the disagreement between the two sets of shift-to-width ratios in columns 7 and 8 is complete, even with liberal error estimates on both groups of results and allowing for the temperature dependence of d/w. Griem's(1964) calculations show d/w as a function of temperature. If one uses these data to estimate the amount of change in d/w in going from 1.6 ev to 2,6 ev, one expects nowhere near as much percentage change in the quantity as there is between Day's and the present results.

CHAPTER 6 - DISCUSSION

A) Estimate of Errors

The errors in the width and shift values in Tables I and II measured by the author contain both systematic and and random error. The tolerances shown were calculated by taking the square root of the sum of the systematic error squared plus the random error squared. For most data, the random error completely outweighed the systematic. We now review how these quantities were estimated.

i) Systematic Errors: It was possible to assess systematic error from the uncertainty in the step filter transmissions, from the inherent inaccuracy and irreproducibility of the transmission readings from the microdensitometer, and from the plate position reading of the comparator stage.

An estimate of the systematic error in the step filter transmissions was obtained through consideration of the uncertainty of the output signal of the calibrating apparatus described on page 43. Here, the noise on the signal constituted an uncertainty much larger than all the others in the technique, and was therefore taken to be the total error. In the worst case studied, namely at a wavelength of 4000Å, the transmissions were good to about 10% on account of the poor sensitivity of the EMI photomultiplier at this wavelength.

However, throughout most of the spectral range of interest, the experimentally determined transmissions could be quoted to ±5%.

The microdensitometer readings were found to be reproducible to ±1%. With errors thus established for both the Datex transmission readings and the step filter transmissions , one could then draw the extreme possibilities that could arise for the "H-D" plot. For any particular line it was then simple to determine graphically how much difference there was between an intensity profile taken from one extreme curve and that taken from the other extreme. Typically, systematic errors on the normalised ordinates of profiles were ±4%.

The comparator stage could be driven with an incremental precision of better than ±1 μ. Thus, considering that all profiles were of the order of 100 μ wide, one needed to allow systematic errors only in the vertical direction on a line profile, In turn, these produced uncertainties in the widths of the standard lines of 0.01Å and of 0.02Å in the plasma line width. The latter figure includes an allowance of ±0.01Å for the uncertainty in the width of the apparatus profile that was deconvolved from the observed to yield the true plasma profile. In the third column of Table I the systematic error of ±0.03Å has been added to the random error to give the total error indicated.

In addition, one expects the aforementioned systematic error in the profile ordinates to produce a spread in the

point on a line profile which the computer chooses as the line centre. One could locate the standard line peaks to no worse than ± 0.005Å and the plasma line peaks to ± 0.01Å. The systematic error in the distance calculated between the standard and reference lines was $\leqslant 0.01$Å while that between the plasma and reference lines $\simeq 0.01$Å. Hence, the systematic error in the difference between these two distances , viz. in the line shift, was taken as ± 0.02Å. The uncertainty estimate in column 6 of Table I contains this estimate of Δd.

ii) Random Errors: The spread that was found in the values of w and d for the four different positions of discharge viewing was attributed to random errors in the experiment. Sources of randomness in the technique were the irreproducibility of the plasma, jitter in the timing of an exposure, differences in exposure that led to use of dissimilar portions of the H-D relation, and the subjectiveness of the choice by the analyst as to which Voigt profile was the best fit to the observed widths.

It would be very difficult to analyse the various contributions to random error. Here we consider the total random error in general terms. The total error in the width is proportional to the width; an approximate figure of $\pm 10\%$ is evidently sufficient to describe the total accuracy. The proportionality is reasonable because the gentler the slope of a line profile, the greater the spread in possible abscissae

that could be read for a given ordinate. Similarly, random processes tended to "smear out" the peak of a line such that the wider a line, the more difficult it was to decide where the centre lay. The whole technique was such that the absolute shift error varied as the width but the percentage error in shift, as the shift-to-width ratio. Having looked at the values of d, Δd, w, Δw, in Table I, one can conclude that the present experimental method is useful for measuring shifts of lines whose d/w is not less than 0.10.

One became quite aware of the random errors while deconvolving the apparatus profile from the observed profiles. It was found that the four profiles of a plasma line taken from the four positions of the discharge column could have different Voigt parameters - some shapes might be close to a true Lorentzian while others would have more Gaussian character. Each line scan was deconvolved according to its own apparent Voigt parameters. The average of the unfolded true halfwidths shown in the tables was taken after the complete Voigt analysis of each scan.

Also, it was found in a number of cases that the profile was not truly Voigt shaped, eg., the .8I and .5I widths taken together would characterize a different Voigt profile than the .7I and .5I widths, say. In such cases, the analyst would average the Voigt parameters to choose a fit intermediate between the extremes suggested by the different widths. This averaging introduced more randomness into the final numbers.

B) The ArII Measurements

The values of the widths in Table I from the present work agree satisfactorily with the results of Roberts(1966) and this is taken as an indication of the correctness of using Jalufka and others'(1966) widths to estimate the electron density. In connexion with the ArII 4132 and ArII 4933 measurements, it is interesting to note that Neufeld(1966) estimated the electron density of essentially the same plasma by scaling the width of the H_α line. Using Griem's(1964) theory of Hydrogen line broadening, he arrived at $n_e = 1.98 \times 10^{17}$ cm^{-3}. Neufeld had reservations about the exactness of the figure because of suspected density gradients in the pulsed-arc. The present work asserts that, on account of the independence of line width on the position of discharge viewed, Abel unfolding is not necessary for the profiles and the H_α width is a valid check on the values presented here for the pure Argon discharge (here, n_e was estimated to be $1.9 \times 10^{17} cm^{-3}$).

On the other hand, agreement in widths and shifts of lines from Multiplets 6, 7 or 14 between theory and experiment is poor, considering either Griem's or other results like those of Roberts(1966) or Cooper and Oertel(1967). These later authors attempt theoretical improvement in several ways: allowing the upper level of interest to interact with many other levels, refinement of the estimate of the strong collision effects, inclusion of higher order terms than dipole in the expansion of the perturbation energy,

allowance for perturbation of the lower level for a transition. While in one or two cases some such modification may bring the theory closer to reality, it appears that in general it lacks the comprehensiveness to make predictions for the ArII widths to better than $\pm 50\%$.

Unfortunately, no shift calculations accompany the aforementioned publications on width, so one cannot criticize the latest theory in this respect. Obviously, Griem's(1964) theory is inadequate. Interestingly, the "Plasma Polarisation Shift" concept leads to numbers that, at best, are only the same order of magnitude as the observed ones. With the present work, the legitimacy of using a time-average potential to represent correlated shift-producing electrons becomes more suspect(see further the discussion by Cooper, 1966).

While the formalism, for obscure reasons, fails to come through with the correct numbers, some of the qualitative predictions are corroborated. In about 60% of all the line deconvolutions, the true profile resulting was very close to the Lorentzian limit, and in the remainder it was closer to the Lorentzian than to the Gaussian. This does indicate that most probably Impact-broadened lines have Lorentzian shapes. The tendency of the plasma conditions and of the timing synchronization to be irreproducible, along with the speed of the Kodak IF emulsion , have meant that several line profiles with some range of characteristics had to be superimposed on a plate for good exposures. Lineshapes thereby suffered

distortion that was not readily analyzable. The approach for determining line shape in this experiment had to be to take a large number (~ 100) of line scans, using only the central parts of profiles. This, in fact, leads to the guarded conclusion above about the shape of the experimental profile.

This experiment anticipates a better one in which the quantum efficiency of the line profile recorder is high enough to require only one plasma discharge for adequate information. The efficiency of the spectroscopic device is indeed the key to checking the line shape: in order to avoid self absorption, in effect one must keep the intensity of the light emitted by the plasma low. In addition to measuring a relatively small photon flux, one will want to record the profile for as short a time as possible. In the present experiment, it is acknowledged that, during the exposure, the intensities of the lines change by 10% and that therefore the plasma parameters are similarly transient. Resulting line images, when five records are taken, each an integral over a finite time and each a little different in its timing, can only be expected to show some variety. A future experiment to record the line profile from a discharge like the pulsed-arc requiring an exposure of only, say, 0.5 μsec during one shot should unequivocally establish the line shape.

Current theory predicts that the asymmetry in line profiles due to ionic broadening should be no greater than 10%. The widths found in this experiment are quoted to $\pm 10\%$, and ,

in fact, no significant asymmetry was observed. Except for the two lines from a special multiplet,(number 32, to be mentioned shortly) it appears that the common width and shift prediction for all members of the same multiplet is substantiated. This characteristic is predicted for the dominant electron broadening, not the ionic broadening, and also is experimentally proven to $\pm 10\%$.

Griem(1964) tabulates Stark parameters only up to Multiplet 10, thus indicating, possibly, that the remainder of that spectrum could not be treated with that theory. In our list of lines, there are some transitions which definitely appear to violate some of the conditions given in chapter 2, part A). It will be useful to mention how these lines are different, and how their data may be used to check enlargements of the theory which consider effects not accounted for earlier.

Multiplet 32 is interesting; in our study, it was represented by the transitions:

4132	$(^1D)4s\,^2D_{3/2}$	-	$(^1D)4p\,^2P^o_{1/2}$
4278	$(^1D)4s\,^2D_{5/2}$	-	$(^1D)4p\,^2P^o_{3/2}$

The values of shift and width given for these lines in Table I are significantly different, as well as being appreciably larger than the same quantities in nearby-numbered multiplets, notably number 31.

ArII 4278 represents a transition that cannot be treated with the Isolated Line assumption because its upper level is

122 cm^{-1} away from an even parity level, $(^1D)3d\,^2D_{5/2}$, in the unperturbed energy level system (Minnhagen, 1963). The plasma frequency in this plasma corresponds to an energy separation of 132 cm^{-1}; since this is approximately the same as the separation between opposite parity levels, we may expect the effect of electron screening of the emitting ions to be important. Thus, a theory to treat the Hydrogenic degeneracy between the levels $(^1D)4p\,^2P^o_{3/2}$ and $(^1D)3d\,^2D_{5/2}$ is required.

Minnhagen(1947) states that the upper level of ArII 4132 is strongly repelled by the $(^1D)3d\,^2D_{3/2}$ level which is only 13 cm^{-1} higher in energy. The half halfwidth of ArII 4132 converted into energy units is 8 cm^{-1} while the shift corresponds to minus 6 cm^{-1}. It therefore appears that the above two interacting states are overlapping. Standard Stark theory requires that when levels suffer perturbation of the order of their zero-order splitting, one must, in general, use the linear theory. Although the approach to overlapping line theory is outlined by Griem et al.(1962), no such calculations exist for ArII transitions. It is suggested here that attempting the calculation for this one unusual line will be worthwhile because a) this is a case where ionic effects may contribute significantly to the shift and is therefore a situation where the understanding of the relative importance of electron and ion processes can be tested, and b) the validity of using LS wave functions (or better ones) can

be examined for these mixed states.

Neufeld(1966) alludes to the possibility of dipole-forbidden lines appearing in the plasma spectrum; such a phenomenon is another aspect of the same situation of perturbed levels. Mixing of the two preceding strongly interacting levels should cause a forbidden line, $(^1D)4s\,^2D_{3/2}$ - $(^1D)3d\,^2D_{3/2}$, to appear at 4129.6Å . This figure is calculated assuming that the $(^1D)3d\,^2D_{3/2}$ level is perturbed positively by 6.1 cm^{-1} , which is the decrease in energy of the $(^1D)4p\,^2P^{\circ}_{1/2}$ state implied by the positive shift of the ArII 4132 line, 1.05Å. On the plates taken by the author for the greatest exposure there was a broad line centred at 4128.5Å which had no partner of like intensity in the standard spectrum and yet whose intensity did increase with increasing percentage of Argon gas in the discharge mixture. No definite claims are made here, however, on the identification and measurement of this line because of its weakness in the present spectra. Again, the advent of a more sensitive profile reading technique should facilitate the evaluation of this interesting possibility.

The fact that the "forbidden line" appears weak in the spectra of the present work is no guarantee that the perturbation calculation of the Stark effects, such as that of Sadjian et al(1961) or Griem(1964), can be used for this transition. It is estimated that the line at 4128.5Å may have 20% of the intensity of the ArII 4132Å line. In this case,

it may be necessary to recalculate the wave functions of the interfering states using a strong field Hamiltonian. If our identification of the line is correct, then the fact that its centre position is significantly different from that calculated in the previous paragraph may be an indication of the need of a better approach than the perturbation treatment. At any rate, Multiplet 32 should be very useful as a test case for nonisolated or overlapping levels theory.

ArII 4104 violates the current theory's requirements in another way: its lower level, $(^3P)4p\,^4D^o_{7/2}$, does suffer appreciable perturbation. To wit, this state is the upper level for the strong line ArII 4348 in Multiplet 7. The usefulness of measuring the ArII 4104 transition is assured because current theory(Cooper and Oertel, 1967) is starting to take lower state polarizability into account. In this case, the amount of broadening of the $(^3P)4p\,^4D^o_{7/2}$ level is now fairly well known experimentally - the chief limitation on the accuracy of the figure for ArII 4348 in Table I is the ignorance of the broadening of the lower level of that line which, Roberts(1966) says, is not negligible. With these data, the theoretician will be able to verify that his calculation for ArII 4104 correctly adds the broadening and shifting of both levels involved in the transition.

Figure 13 shows the large widths and shifts of the lines in Multiplets 32 and 52. The very weak "forbidden" line image is at a scale reading of 10.53 .

C) The NII Measurements

Looking at Table II, one has to conclude that agreement between the different experimental results of width and shift measurement in NII is hardly outstanding. It does appear that something went wrong with Day's measurement of the three narrow lines NII5045, NII 4614 and NII 5496. The disagreement between Berg and others'(1967) results for widths and the present ones is small enough to be put down to temperature dissimilarity. The disparity between those two sets of data and Day's cannot be thus explained. The error estimates given in all three experiments seem to be of reasonable size, considering the techniques used, and this argues against poor sampling.

It should be remarked that the widths of the first three lines in Table II stand in the same ratio among themselves in Day's work as in the present and this suggests that his electron density calibration , done by scaling the halfwidth of the HeI 3889 line, may be in error. For instance, in similar T-tube plasmas (eg. James, 1965), it has been found that HeI 3889 is not dependable for line profile measurements because of a fairly bright impurity line, CIII 3889, in its blue wing. Day also voices dissatisfaction with the use of the HeI 3889 profile as a density probe because the Stark parameters are not well known from experiment. On the other hand, the n_e estimate in the present work, which was done by

comparing measured ArII widths with other experimental results, is defended as realistic because the present widths check out with scaled widths from independent work on ArII by Roberts(1966), who used a laser - interferometer technique for the n_e determination, and from work on NII by Berg et al (1967), who estimated n_e from the width of a HeI line.

The widths of the last three lines in Table II show agreement between Berg and others' work and the present. While little can be said about the values in columns 4 and 6 for all six transitions, Griem's(1966) theoretical estimates in column 6 give little assurance that the broadening processes are well understood when compared with the numbers in columns 3 and 5.

For the last three transitions in the table, the experimental shift-to-width ratios do all agree, even though the percentage error in these quantities is very large. The different authors' work together puts limits on the ratios which leads to the useful information that the shift-to-width value is no larger than a comparatively small(~0.01) number. This is in contrast with the ArII character where broad lines also have big shifts. Here too, the three sets of d/w values remind one that, no matter what the technique, the wider the line the more difficult it is to decide where its centre is, and thus the greater the uncertainty in the measured shift.

D) Conclusion

Some lines in the ArII and NII spectra emitted by a dense plasma have been measured for width and shift using a photographic technique. It has been found that the width results agree well with those from some other experiments, and that there remains at least a 20% discrepancy between these and theoretical values. The work is one of the first in extensive ArII shift measurement and, as such, has little available for comparison in other experiment. The ArII and NII shift theories seem to be totally inadequate.

The width measuring technique is sufficiently accurate in the light of the present quantitative theory. The next step in researching Stark profiles should involve a device to accurately measure the line profile and peremptorily establish its shape. In the current calculations, the electron impacts give the Lorentzian shape to the centre of the line profile while the far wings characterize the ionic broadening. But the demarcation between the extremities is not sharp, and the question of how to calculate the intensity profile for the intermediate frequencies should now be regarded by theoreticians as an important one. So then, an experimental determination of the precise form of $I(\omega)$ which correctly contains even the far wings will be a great boon in testing the understanding of the relative importances of the different perturbations.

It is possible that the NII widths produced by Day(1965)

suffer from a poor n_e calibration. His shift-to-width ratios, however, should have no such troubles since this quantity ought to depend only on the plasma temperature. Certainly, on the plates measured by the present author, lines with a d/w of the order of 1 stood out rather spectacularly - one needed merely to examine the plates by eye to appreciate them. None of the thre narrow NII lines in the group studied were seen to thus distinguish themselves. Herein we see the great convenience in the technique of putting the standard and plasma spectra side by side on the same plate: our identification of the plasma line was quickly determined from the identification of the standard line beside it. The approximate size of the d/w value to be expected was noted at the same time. Monochromator - photomultiplier systems do not normally allow of these safety features.

Technologically, the measurement of shift seems to have advanced to satisfactory state with this work, considering the state of the theory. One can determine shifts even more easily than in the present method if one does not need to read widths from the photographic records, because then time need not be spent in making sure that the plasma is optically thin and that the photographic technique is correctly used, as in the measurement of line profiles. Thus, the comparatively easy method of using shifts rather than widths for gauging electron density commends itself to the experimentalist.

In summary, the experiment has been successful in quantitative measurements. Hopefully, it will not be too long before theoreticians are inspired to improve at least the NII and ArII calculations. It would be interesting to see the problems of Debye shielding(nonisolated lines) and of overlapping and forbidden lines in these spectra attended to. The general understanding of three body physics, as required in the treatment of the above situations, will prosper, it is hoped, by the measurements submitted herewith.

BIBLIOGRAPHY

Baranger, M. (1962), in "Atomic and Molecular Processes" (D. R. Bates, ed.), 493 (New York; Academic Press).

Bates, D. R., and Damgaard, A. (1950), Phil. Trans. Roy. Soc. A242, 101.

Berg, H. F., Ervens, W., and Furch, B. (1967), Z. Physik 206, 309.

Breene, R. G. (1961), "The Shift and Shape of Spectral Lines" (New York; Pergamon Press).

Burgess, D. D., and Cooper, J. (1965a), Proc. Phys. Soc. 85, 1261.

Burgess, D. D., and Cooper, J. (1965b), J. Sci. Instr. 42, 829.

Condon, E. U., and Shortley, G. H. (1935), "The Theory of Atomic Spectra" (London; Cambridge University Press).

Cooper, J. (1966), Rep. Prog. Phys. 29, 35.

Cooper, J., and Oertel, G. K. (1967), Phys. Rev. Letters 18, 985.

Day, R. A., (1965), Ph.D. Thesis, University of Maryland.

Durand, J. (1963), Z. Naturforsch. 18a, 281.

Erfle, H. (1924), in "Grundzuge der Theorie der Optischen Instrumente" (Czapski and Epstein, ed.), 320 (Leipzig; Barth).

Eriksson, K. B. S. (1958), Ark. Fys. 13, 303.

Griem, H. R. (1964), "Plasma Spectroscopy" (New York; McGraw Hill).

Griem, H. R. (1966), Phys. Rev. Letters 17, 509.

Griem, H. R., Baranger, M., Kolb, A. C., and Oertel, G. (1962), Phys. Rev. 125, 177.

Heitler, W. (1954), "The Quantum Theory of Radiation" (London; Oxford University Press).

Jalufka, N. W., Oertel, G. K., and Ofelt, G. S. (1966), Phys. Rev. Letters 16, 1073.

James, H. G. (1965), M.Sc. Thesis, University of British Columbia.

Kodak (1962), "Kodak Plates and Films for Science and Industry" Kodak publication P-9 (Rochester; Eastman Kodak).

Margenau, H., and Lewis, M. (1959), Rev. Mod. Phys. 31, 569.

Mees, C. E. K., and James, T. H. (1966), "The Theory of the Photographic Process" (New York; Macmillan).

Minnhagen, L. (1947), Ark. Mat. Ast. Fys. 35A, No.16 .

Minnhagen, L. (1963), Ark. Fys. 25, 203.

Minnhagen, L. (1964), J. Res. of N.B.S. 68C, 337.

Moore, C. E. (1959), "A Multiplet Table of Astrophysical Interest" N.B.S. Tech. Note 36.

Neufeld, C. R. (1966), Ph.D. Thesis, University of British Columbia.

Olsen, H. N. (1963), J. Quant. Spectr. Rad. Transfer 3, 59.

Popenoe, C. H., and Shumaker, J. B. jr. (1965), J. Res. of N.B.S. 69A, 495.

Roberts, D. E. (1966), Phys. Letters 22, 417.

Sadjian, H., Wimmel, H. K., and Margenau, H. (1962), J. Quant. Spectr. Rad. Transfer 1, 46.

Theophanis, G. A. (1960), Rev. Sci. Instr. 31, 427.

Tompkins, F. S., and Fred, M. (1951), J. Opt. Soc. Am. 41, 641.

Traving, G. (1960), "Uber die Theorie der Druckverbreiterung von Spektrallinien" (Karlsruhe; G. Braun).

Van de Hulst, H. C., and Reesinck, J. J. M. (1947), Astrophys. J. 106, 121.

Unsold, A. (1938), "Physik der Sternatmospharen" (Berlin; Springer).

Wiese, W. L. (1965), in "Plasma Diagnostic Techniques" (Huddlestone and Leonard, ed.), 265 (New York;Academic Press).